Since GFAP is expressed as a result of gliosis and hypertrophy of macroglial cells, it is a common marker of pathological or stressful conditions in astrocytes and Müller cells in the retina (Hartig et al. 1995; Reichenbach and Reichelt 1986). Kimura et al. (2000) showed that the immunoreactivity of GFAP in RCS rats begins at P35 and continues until P105. In this study, we demonstrated that GFAP immunoreactivity was strong in Müller cells 3 months after the birth and continued for more than a year. Similarly, increased GFAP immunoreactivity also has been observed in the rd mouse model of photoreceptor degeneration (Strettoi et al. 2003) and in glaucoma models that caused the death of RGCs (Schuettauf et al. 2004; Tezel et al. 2003). The increased immunoreactivity might be due to stress responses that are associated with the degeneration of photoreceptors, second order neurons, or Müller cells. We observed decreased GFAP immunoreactivity in ChR2V-expressing RGCs. Dai et al. (2011) recently reported that GFAP protein expression increased in Müller cells during the death of RGCs caused by the experimental glaucoma model and the GFAP expression was inhibited by the rescue of RGCs death. The activation of astroglia or Müller cells coincides with the degeneration of RGCs (Bosco et al. 2008; Schmidt et al. 2007; Schuettauf et al. 2004; Tezel et al. 2003). Taken together with our previous report that VEPs could be maintained for up to 64 weeks after the *ChR2* transduction (Sugano et al. 2010; Tomita et al. 2010), ChR2V may inhibit secondary degeneration of RGCs in the retina. Although the mechanism of this protection is not known, ChR2V may stimulate RGCs or neurotrophic factors. For example, it is known that electrical stimulation of the retina prevents secondary degeneration (Schmid et al. 2009) and axotomy-induced RGC death (Morimoto et al. 2002, 2005, 2010). Similarly, depolarization and elevation of intracellular cAMP in RGCs increase the levels of brain-derived neurotrophic factor (BDNF) receptor trkB, which prevents RGC cell death because BDNF acts as a survival factor for RGCs (Meyer-Franke et al. 1998; Shen et al. 1999) Further study is needed to elucidate the mechanism of the antidegenerative effects of ChR2.

In conclusion, our results showed that although the number of RGCs decreased during photoreceptor degeneration, the activity of individual RGCs was preserved. In addition, *ChR2* transduction can produce photosensitive RGCs in both young and aged rats. However, the degree of recovery depended on their age at the time of transduction.

Grant support This work was partly supported by Grants-in-Aid for Scientific Research from the Ministry of Education, Culture, Sports, Science and Technology of Japan (No. 21791664 and 21200022); Science and Culture and Special Coordination Funds for Promoting Science and Technology of the Japanese Government, Strategic Research Program for Brain Sciences (SRPBS); Ministry of Health, Labour and Welfare of Japan; Japan Foundation for Aging and Health; and the Program for Promotion of Fundamental Studies in Health Sciences of the National Institute of Biomedical Innovation (NIBIO).

References

Ali RR, Reichel MB, De Alwis M et al (1998) Adeno-associated virus gene transfer to mouse retina. Hum Gene Ther 9:81–86

Bi A, Cui J, Ma YP et al (2006) Ectopic expression of a microbial-type rhodopsin restores visual responses in mice with photoreceptor degeneration. Neuron 50:23–33

Bosco A, Inman DM, Steele MR et al (2008) Reduced retina microglial activation and improved optic nerve integrity with minocycline treatment in the DBA/2J mouse model of glaucoma. Invest Ophthalmol Vis Sci 49:1437–1446

Bowes C, Li T, Danciger M, Baxter LC, Applebury ML, Farber DB (1990) Retinal degeneration in the rd mouse is caused by a defect in the beta subunit of rod cGMP-phosphodiesterase. Nature 347:677–680

Boyden ES, Zhang F, Bamberg E, Nagel G, Deisseroth K (2005) Millisecond-timescale, genetically targeted optical control of neural activity. Nat Neurosci 8:1263–1268

Brecha NC, Weigmann C (1994) Expression of GAT-1, a high-affinity gamma-aminobutyric acid plasma membrane transporter in the rat retina. J Comp Neurol 345:602–611

Bush RA, Hawks KW, Sieving PA (1995) Preservation of inner retinal responses in the aged Royal College of Surgeons rat. Evidence against glutamate excitotoxicity in photoreceptor degeneration. Invest Ophthalmol Vis Sci 36:2054–2062

Dai Y, Weinreb RN, Kim KY et al (2011) Inducible nitric oxide synthase-mediated alteration of mitochondrial OPA1 expression in ocular hypertensive rats. Invest Ophthalmol Vis Sci 52:2468–2476

Grunder T, Kohler K, Guenther E (2001) Alterations in NMDA receptor expression during retinal degeneration in the RCS rat. Vis Neurosci 18:781–787

Hartig W, Grosche J, Distler C, Grimm D, El-Hifnawi E, Reichenbach A (1995) Alterations of Muller (glial) cells in dystrophic retinae of RCS rats. J Neurocytol 24:507–517

Humayun MS, Prince M, de Juan E Jr et al (1999) Morphometric analysis of the extramacular retina from postmortem eyes with retinitis pigmentosa. Invest Ophthalmol Vis Sci 40:143–148

Huxlin KR, Goodchild AK (1997) Retinal ganglion cells in the albino rat: revised morphological classification. J Comp Neurol 385:309–323

Ishizuka T, Kakuda M, Araki R, Yawo H (2006) Kinetic evaluation of photosensitivity in genetically engineered neurons expressing green algae light-gated channels. Neurosci Res 54:85–94

Kimura N, Nishikawa S, Tamai M (2000) Muller cells in developing rats with inherited retinal dystrophy. Tohoku J Exp Med 191:157–166

LaVail MM, Battelle BA (1975) Influence of eye pigmentation and light deprivation on inherited retinal dystrophy in the rat. Exp Eye Res 21:167–192

Marc RE, Jones BW, Watt CB, Strettoi E (2003) Neural remodeling in retinal degeneration. Prog Retin Eye Res 22:607–655

Marc RE, Jones BW, Anderson JR et al (2007) Neural reprogramming in retinal degeneration. Invest Ophthalmol Vis Sci 48:3364–3371

Martin KR, Klein RL, Quigley HA (2002) Gene delivery to the eye using adeno-associated viral vectors. Methods 28:267–275

McLaughlin ME, Sandberg MA, Berson EL, Dryja TP (1993) Recessive mutations in the gene encoding the beta-subunit of rod phosphodiesterase in patients with retinitis pigmentosa. Nat Genet 4:130–134

Meyer-Franke A, Wilkinson GA, Kruttgen A et al (1998) Depolarization and cAMP elevation rapidly recruit TrkB to the plasma membrane of CNS neurons. Neuron 21:681–693

Morimoto T, Miyoshi T, Fujikado T, Tano Y, Fukuda Y (2002) Electrical stimulation enhances the survival of axotomized retinal ganglion cells in vivo. Neuroreport 13:227–230

Morimoto T, Miyoshi T, Matsuda S, Tano Y, Fujikado T, Fukuda Y (2005) Transcorneal electrical stimulation rescues axotomized retinal ganglion cells by activating endogenous retinal IGF-1 system. Invest Ophthalmol Vis Sci 46:2147–2155

Morimoto T, Miyoshi T, Sawai H, Fujikado T (2010) Optimal parameters of transcorneal electrical stimulation (TES) to be neuroprotective of axotomized RGCs in adult rats. Exp Eye Res 90:285–291

Mullen RJ, LaVail MM (1976) Inherited retinal dystrophy: primary defect in pigment epithelium determined with experimental rat chimeras. Science 192:799–801

Nagel G, Szellas T, Huhn W et al (2003) Channelrhodopsin-2, a directly light-gated cation-selective membrane channel. Proc Natl Acad Sci USA 100:13940–13945

Pavlidis M, Fischer D, Thanos S (2000) Photoreceptor degeneration in the RCS rat attenuates dendritic transport and axonal regeneration of ganglion cells. Invest Ophthalmol Vis Sci 41:2318–2328

Pu M, Xu L, Zhang H (2006) Visual response properties of retinal ganglion cells in the royal college of surgeons dystrophic rat. Invest Ophthalmol Vis Sci 47:3579–3585

Reichenbach A, Reichelt W (1986) Postnatal development of radial glial (Muller) cells of the rabbit retina. Neurosci Lett 71:125–130

Santos A, Humayun MS, de Juan E Jr et al (1997) Preservation of the inner retina in retinitis pigmentosa. A morphometric analysis. Arch Ophthalmol 115:511–515

Sato H, Tomita H, Nakazawa T, Wakana S, Tamai M (2005) Deleted in polyposis 1-like 1 gene (Dp111): a novel gene richly expressed in retinal ganglion cells. Invest Ophthalmol Vis Sci 46:791–796

Sauve Y, Lu B, Lund RD (2004) The relationship between full field electroretinogram and perimetry-like visual thresholds in RCS rats during photoreceptor degeneration and rescue by cell transplants. Vision Res 44:9–18

Schmid H, Herrmann T, Kohler K, Stett A (2009) Neuroprotective effect of transretinal electrical stimulation on neurons in the inner nuclear layer of the degenerated retina. Brain Res Bull 79:15–25

Schmidt JF, Agapova OA, Yang P, Kaufman PL, Hernandez MR (2007) Expression of ephrinB1 and its receptor in glaucomatous optic neuropathy. Br J Ophthalmol 91:1219–1224

Schuettauf F, Rejdak R, Walski M et al (2004) Retinal neurodegeneration in the DBA/2J mouse-a model for ocular hypertension. Acta Neuropathol 107:352–358

Shen S, Wiemelt AP, McMorris FA, Barres BA (1999) Retinal ganglion cells lose trophic responsiveness after axotomy. Neuron 23:285–295

Sineshchekov OA, Jung KH, Spudich JL (2002) Two rhodopsins mediate phototaxis to low- and high-intensity light in Chlamydomonas reinhardtii. Proc Natl Acad Sci USA 99:8689–8694

Stone JL, Barlow WE, Humayun MS, de Juan E Jr, Milam AH (1992) Morphometric analysis of macular photoreceptors and ganglion cells in retinas with retinitis pigmentosa. Arch Ophthalmol 110:1634–1639

Strettoi E, Pignatelli V (2000) Modifications of retinal neurons in a mouse model of retinitis pigmentosa. Proc Natl Acad Sci USA 97:11020–11025

Strettoi E, Porciatti V, Falsini B, Pignatelli V, Rossi C (2002) Morphological and functional abnormalities in the inner retina of the rd/rd mouse. J Neurosci 22:5492–5504

Strettoi E, Pignatelli V, Rossi C, Porciatti V, Falsini B (2003) Remodeling of second-order neurons in the retina of rd/rd mutant mice. Vision Res 43:867–877

Sugano E, Tomita H, Ishiguro S, Abe T, Tamai M (2005) Establishment of effective methods for transducing genes into iris pigment epithelial cells by using adeno-associated virus type 2. Invest Ophthalmol Vis Sci 46:3341–3348

Sugano E, Isago H, Wang Z, Hiroi T, Tamai M, Tomita H (2010) Immune responses to adeno-associated virus type 2 encoding channelrhodopsin-2 in a genetically blind rat model for gene therapy. Gene Therapy 18:266–274

Tamai M, Chader GJ (1979) The early appearance of disc shedding in the rat retina. Invest Ophthalmol Vis Sci 18:913–917

Tezel G, Chauhan BC, LeBlanc RP, Wax MB (2003) Immunohistochemical assessment of the glial mitogen-activated protein kinase activation in glaucoma. Invest Ophthalmol Vis Sci 44:3025–3033

Tomita H, Kotake Y, Anderson RE (2005) Mechanism of protection from light-induced retinal degeneration by the synthetic antioxidant phenyl-N-tert-butylnitrone. Invest Ophthalmol Vis Sci 46:427–434

Tomita H, Sugano E, Yawo H et al (2007) Restoration of visual response in aged dystrophic RCS rats using AAV-mediated channelopsin-2 gene transfer. Invest Ophthalmol Vis Sci 48:3821–3826

Tomita H, Sugano E, Fukazawa Y et al (2009) Visual properties of transgenic rats harboring the channelrhodopsin-2 gene regulated by the thy-1.2 promoter. PLoS One 4:e7679

Tomita H, Sugano E, Isago H et al (2010) Channelrhodopsin-2 gene transduced into retinal ganglion cells restores functional vision in genetically blind rats. Exp Eye Res 90:429–436

Tsuda M, Glaccum M, Nelson B, Ebrey TG (1980) Light isomerizes the chromophore of bacteriorhodopsin. Nature 287:351–353

ARTICLE

BIOTECHNOLOGY and BIOENGINEERING

Optically Controlled Contraction of Photosensitive Skeletal Muscle Cells

Toshifumi Asano,[1,2] Toru Ishizua,[1,3] Hiromu Yawo[1,3,4,5]

[1]Department of Developmental Biology and Neuroscience, Tohoku University Graduate School of Life Sciences, Sendai, Japan; telephone: +81-22-217-6208; fax: +81-22-217-6211; e-mail: yawo-hiromu@m.tohoku.ac.jp

[2]Japan Society for the Promotion of Science, Chiyoda, Tokyo, Japan

[3]Japan Science and Technology Agency (JST), Core Research of Evolutional Science & Technology (CREST), Tokyo, Japan

[4]Tohoku University Basic and Translational Research Center for Global Brain Science, Sendai, Japan

[5]Center for Neuroscience, Tohoku University Graduate School of Medicine, Sendai, Japan

Received 19 April 2011; revision received 8 July 2011; accepted 25 July 2011

Published online 1 August 2011 in Wiley Online Library (wileyonlinelibrary.com). DOI 10.1002/bit.23285

ABSTRACT: As the skeletal muscle cell is an efficient force transducer, it has been incorporated in bio-microdevices using electrical field stimulation for generating contractile patterns. To improve both the spatial and temporal resolutions, we made photosensitive skeletal muscle cells from murine C2C12 myoblasts, which express channelrhodopsin-2 (ChR2), one of archaea-type rhodopsins derived from green algae *Chlamydomonas reinhardtii*. The cloned ChR2-expressing C2C12 myoblasts were made and fused with untransfected C2C12 to form multinucleated myotubes. The maturation of myotubes was facilitated by electrical field stimulation. Blue LED light pulse depolarized the membrane potential of a ChR2-expressing myotube and eventually evoked an action potential. It also induced a twitch-like contraction in a concurrent manner. A contraction pattern was thus made with a given pattern of LED pulses. This technique would have many applications in the bioengineering field, such as wireless drive of muscle-powered actuators/microdevices.

Biotechnol. Bioeng. 2012;109: 199–204.

KEYWORDS: optical stimulation; channelrhodopsin; C2C12; myotube; myoblast; muscle contraction

Introduction

Bio-microdevices incorporating biological components such as tissues, cells, and biomolecules have raised much attention for the development of novel engineering devices. Muscle cells could provide force-generating modules driven by the activation of actin–myosin motors coordinated with excitation–contraction coupling (Bers, 2002). As an efficient force transducer, a muscle-powered micro-actuator driven by biochemical energy reaction could save energy, resources, and space. With these advantages, contractile muscles have been incorporated into engineered bio-microdevices to create motors, actuators (Feinberg et al., 2007; Kim et al., 2007; Morishima et al., 2006; Wilson et al., 2010; Xi et al., 2005), and pumps (Tanaka et al., 2007). Conventionally, muscle contraction has been triggered by electrical field stimulation using electrodes placed in the extracellular space. Alternatively, spontaneously beating cardiac muscle cells have also been used. Electrical field stimulation is a simple method to control the temporal pattern of contractile activity. However, the electrical field is generally non-uniform and many unexpected muscle cells are stimulated simultaneously. It is thus difficult to specifically stimulate identified groups of muscle cells.

The optical stimulation methods have raised much attention recently because of their advantages over conventional electrical stimulation methods: Fine resolution in space and time, parallel stimulations at multiple sites, relative harmlessness and convenience (Callaway and Yuste, 2002; Miesenböck, 2004). Recently, photostimulation using channelrhodopsin-2 (ChR2), which are involved in the light-dependent behavior of a unicellular green alga, *Chlamydomonas reinhardtii* (Nagel et al., 2003), has become a powerful tool for the investigation of neural networks in vivo and in vitro (Boyden et al., 2005; Ishizuka et al., 2006; Li et al., 2005).

In this study, to render contractile muscle photosensitive, one of the mouse muscle sarcoma cell lines, C2C12 myoblast

Correspondence to: H. Yawo

Contract grant sponsor: Ministry of Education, Culture, Sports, Science and Technology (MEXT) of Japan

Additional supporting information may be found in the online version of this article

(Yaffe and Saxel, 1977), is genetically engineered to express ChR2. The C2C12 myoblasts are fused with each other in vitro, becoming contractile with the formation of myofibrils, and are applied to study skeletal muscle cell physiology (Fujita et al., 2007; Nakanishi et al., 2007; Nedachi and Kanzaki, 2006; Yamaguchi et al., 2010) or contractive mechanics (Kaji et al., 2010; Nagamine et al., 2011; Yamasaki et al., 2009). We found that patterned contraction of ChR2-expressing myotubes was robustly triggered by blue LED light. Optical stimulation techniques with the combination of ChR2-expressing C2C12 myoblasts and microfabrication could enable wireless manipulation of muscle-powered actuators/microdevices.

Materials and Methods

Cell Culture and Generation of ChR2-Venus-Transfected C2C12 Cell Lines

Murine C2C12 myoblasts were obtained from RIKEN Cell Bank (RCB0987) and cultured at 37°C under a 5% CO_2 atmosphere in Dulbecco's Modified Eagle's Medium (DMEM, Sigma–Aldrich, St. Louis, MO) supplemented with 10% Fetal Bovine Serum (FBS, Biological Industries Ltd), 100 units/mL penicillin, 100 μg/mL streptomycin (Sigma–Aldrich). A murine leukemia virus-based vector, SRα-chop2-Venus, was constructed by replacing enhanced green fluorescent protein (EGFP) in SRαLEGFP with ChR2 apoprotein tagged with a modified yellow fluorescent protein, Venus (Nagai et al., 2002), and the pseudovirions were prepared as described previously (Kamada et al., 2004). The titer of the virus stock was 1.4×10^5 infectious particles per mL. To generate ChR2-Venus expressing stable lines, C2C12 cells were transfected with the virions and cloned twice by limited dilution. Single-cell clones with bright Venus fluorescence were selected under the conventional inverted-fluorescent microscopy.

Formation and Maturation of Myotubes

Once confluent, the C2C12 myoblasts were induced to differentiate into myotubes in the differentiation medium consisting of DMEM supplemented with 2% calf serum (Thermo Fisher Scientific, Waltham, MA), 1 nM insulin (Invitrogen, Carlsbad CA), 100 units/mL penicillin, and 100 μg/mL streptomycin, which was replaced every 24 h. To facilitate the maturation of myotubes, they were transferred to electrical field stimulation medium, which was composed of DMEM supplemented with 2% calf serum, 2% MEM amino acid solution (Invitrogen), 1% MEM non-essential amino acid solution (Invitrogen), 100 units/mL penicillin, and 100 μg/mL streptomycin. Electrical pulses (0.8 V/mm, 2 ms duration) were generated by a pulse generator (SEN-7203, Nihon Kohden, Tokyo, Japan) and applied at 1 Hz continuously for 3 days through bipolar carbon electrode plates. The electrical field stimulation medium was changed every 12 h during each stimulation protocol.

Electrophysiology

Fluorescence-labeled myotubes were identified under conventional epi-fluorescence microscopy (BH2-RFC, Olympus, Tokyo, Japan) equipped with a 60× water-immersion objective (LUMplanPl/IR60x, Olympus). The photocurrents were recorded as described previously (Ishizuka et al., 2006) under the whole-cell patch clamp of a conventional system (Axopatch 200A plus Digidata1200, Molecular Devices Co.). The standard patch pipette solution contained (in mM): 40 KCl, 80 KCH_3SO_4, 10 HEPES, 1 $MgCl_2$, 2.5 MgATP, 0.2 Na_2EGTA (pH 7.4 adjusted with KOH). The standard extracellular solution contained (in mM): 138 NaCl, 3 KCl, 1 $CaCl_2$, 1 $MgCl_2$, 10 HEPES, 4 NaOH (pH 7.4 adjusted with HCl). All the experiments were carried out at room temperature.

Immunocytochemistry

The cultured myotubes were washed with PBS and fixed for 15 min in 0.1 M PBS (pH 7.4) containing 4% paraformaldehyde (PFA) and 0.1% Triton X-100. The specimens were blocked in PBS with 5% donkey serum for 1 h and reacted with mouse monoclonal anti-sarcomeric α-actinin primary antibody (1:400; Sigma–Aldrich) in PBS with 5% donkey serum and 0.1% Triton X-100 for 1 h. After washing three times in PBS with 0.1% Triton X-100, the cells were incubated for 1–2 h with the Alexa Fluor 546-conjugated anti-mouse IgG secondary antibody in PBS with 5% donkey serum and 0.1% Triton X-100. Alexa Fluor 633-labeled phalloidin was added to the secondary antibody solution to visualize the filamentous actin (F-actin). All of the above reactions were done at room temperature. The specimens were mounted with Vectashield (Vector Laboratories, Burlingame, CA) and coverslipped. The fluorescent images were taken under conventional confocal laser microscopy (LSM510META, Carl Zeiss, Oberkochen, Germany) equipped with a 40× objective and corrected for brightness and contrast using conventional software (LSM Image Browser).

Optical Stimulation and Motion Analysis

Optical stimulation was carried out by blue LED (470 ± 25 nm, LXHL-NB98, Philips Lumileds Lighting Inc. San Jose, CA) regulated by a pulse generator (SEN-7203, Nihon Kohden) with a current booster (SEG-3104, Nihon Kohden) in a high-calcium extracellular solution (in mM, 138 NaCl, 3 KCl, 10 HEPES, 4 NaOH, 1.25 $MgCl_2$, 10 $CaCl_2$, pH 7.4 adjusted with HCl). Its light power density was directly measured by a thermopile (MIR-100Q, Mitsubishi Oil Chemicals, Tokyo, Japan) and was 0.12

mW/mm^2 at the bottom of the culture dish. Each photostimulation protocol was given with an interval of 3–5 min. The contractile movements of myotubes were monitored by a CCD camera (VB-7010, Keyence Co., Osaka, Japan; 7.5 frames/s) under phase-contrast microscopy. Each sequential image was converted to gray scale, inverted in brightness, and the point of maximal pixel value was identified in the region of interest covering the myotube. The contractile displacement was measured by tracking this point, and expressed in μm after correcting the scale. All the above image analyses were carried out using ImageJ software (NIH, Bethesda, MD).

Results and Discussions

Formation of C2C12 Myotubes Expressing ChR2

Probably due to repeated passage before establishing the cloned myoblasts which stably express ChR2 (ChR2-C2C12), they did not form well-differentiated myotubes. Since the C2C12 cells fused with each other and formed multi-nucleated myotubes (Blau et al., 1983), this genetic deficit was expected to be overcome by fusion with untransfected C2C12 (UT-C2C12) cells. Therefore, we co-cultured ChR2-C2C12 cells with UT-C2C12 cells in the ratio of 1:2 and rendered them to be fused with each other. As shown in Fig. 1A the multi-nucleated myotubes expressing ChR2-Venus were almost similar to those from UT-C2C12 cells in gross appearance. Under confocal microscopy, ChR2-Venus was distributed uniformly at the contour of the multi-nucleated myotube, suggesting that it was localized in the plasma membrane (Fig. 1B). Among multi-nucleated myotubes, about 80% were expressed ChR2-Venus. Therefore, the ChR2-C2C12 cells appear to be fused with the UT-C2C12 cells to form multi-nucleated myotubes with the diffusion of ChR2-Venus molecules along their plasma membranes.

Photocurrents were evoked by 100 ms blue LED light pulses of variable strength under whole-cell patch clamp of the multi-nucleated myotube expressing ChR2-Venus (Fig. 2A). The blue LED light induced a negative current with a peak and a plateau at a holding potential of −60 mV, as reported previously (Ishizuka et al., 2006). Both the peak and plateau currents were dependent on the light intensity. Under current-clamp, the resting potential was between −50 and −30 mV ($n = 7$) and action potentials were not evoked even by direct current injection. When hyperpolarized to around −70 mV, the blue LED light pulse evoked membrane depolarization and, eventually, an action potential similar to that by the direct current injection (Fig. 2B). However, the light-evoked action potential frequently failed to be evoked even at the maximal strength (0.08 mW/mm^2) and no action potential was evoked in two myotubes. In another two myotubes, each depolarization, either electrically or optically, was sometimes accompanied with contraction, but frequently was not.

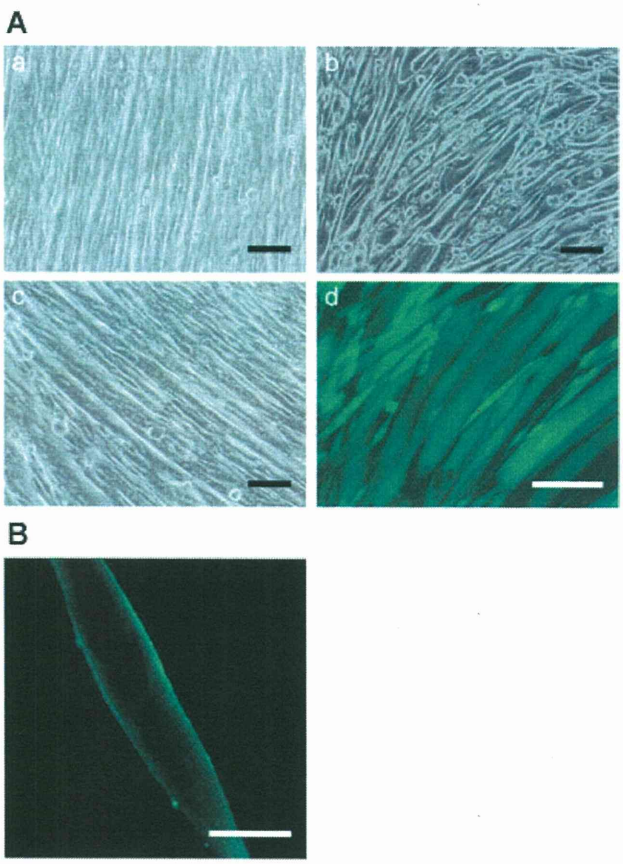

Figure 1. ChR2-expressing C2C12 myotubes. **A**: Phase-contrast images of multinucleated myotubes cultured in the differentiation medium for 10 days; (**a**) from untransfected (UT)-C2C12, (**b**) from C2C12 cells which stably expressed ChR2 (ChR2-C2C12), (**c**) from co-cultured ChR2-C2C12 with UT-C2C12 in the ratio of 1:2 and (**d**) Venus-fluorescence images of co-cultured myotubes. Note that some of them expressed ChR2-Venus conjugates. **B**: A confocal image of typical multi-nucleated myotubes expressing ChR2-Venus conjugates. Scale bars: 100 μm in A, 20 μm in B. [Color figure can be seen in the online version of this article, available at http://wileyonlinelibrary.com/bit]

Maturation of Myotubes

Under conventional differentiation conditions, the development of sarcomere structure in a C2C12 myotube is very slow and its contractile activity is also retarded (Engler et al., 2004). However, it has been reported that the electrical field stimulation evoked membrane depolarization, transiently increased the intracellular Ca^{2+}, accelerated the sarcomere assembly, and facilitated the contractile activity in the C2C12 myotube (Fujita et al., 2007). Before applying the electrical field stimulation protocol, the sarcomeric structure, which is the smallest contractile unit, was not obvious in the C2C12 myotubes (Fig. 3A). On the other hand, after 3-day application of the electrical field stimulation protocol (0.8 V/mm, 2 ms pulse at 1 Hz), which was given by electrodes placed in the culture dish, striation patterns consisting of sarcomeric α-actinin and F-actin were manifest in the C2C12 myotubes (Fig. 3B). The sarcomeric

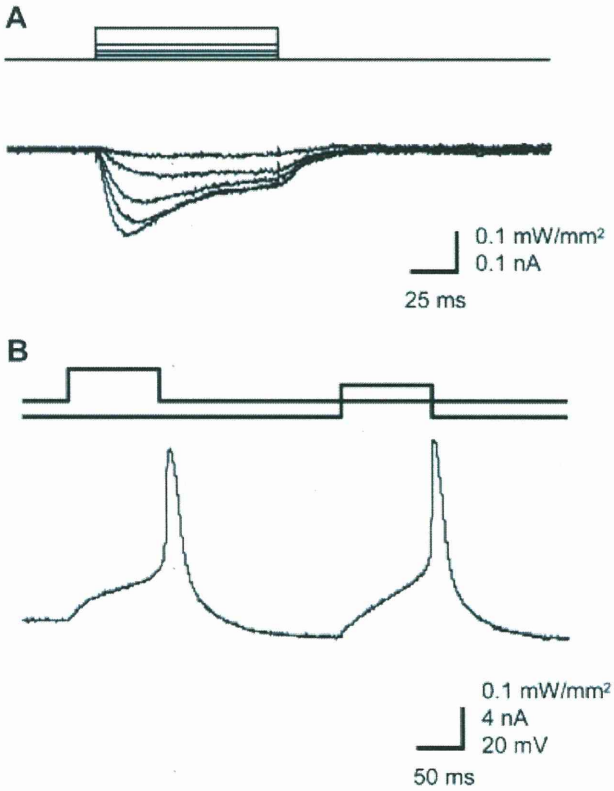

Figure 2. Optical stimulation of ChR2-expressing C2C12 myotube. **A**: Top, blue LED light pulses and bottom, photocurrent responses of a multi-nucleated myotube from ChR2-C2C12 co-cultured with UT-C2C12. **B**: Top, blue LED light pulse, middle, current injection from the patch electrode, and bottom, a typical membrane potential response. Resting potential, −67 mV.

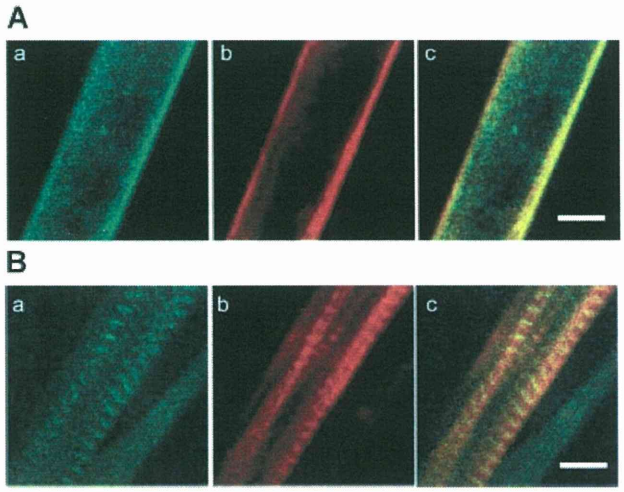

Figure 3. Maturation of sarcomeric structures. **A**: The ChR2-expressing C2C12 myotube before applying the electrical field stimulation protocol. **a**: Distribution of anti-α-actinin immunoreactivity (green). **b**: Distribution of F-actin indicated by Alexa Fluor 633-labeled phalloidin. **c**: Merged image of (a) and (b). **B**: The maturated myotube after 3-day application of electrical filed stimulation protocol with similar panels (**a**)–(**c**) as in (A). Scale bars: 10 μm.

structure appeared to be prominently localized in a banded pattern which ran in a longitudinal direction along each myotube. These results were consistent with those of previous studies (Fujita et al., 2007; Nagamine et al., 2010), and the periodic electrical stimulation efficiently facilitated the assembly of sarcomeric structures.

Contractile Activity Controlled by Optical Stimulation

After 3-day electrical field stimulation, the contractile activity of the ChR2-Venus-expressing myotubes was examined using optical stimulation by blue LED (0.12 mW/mm^2, 100 ms duration) and electrical field stimulation (0.8 V/mm, 100 ms duration). Typically, these myotubes showed obvious contraction synchronous to each light or electric pulse of a given frequency (Supplementary Movie S1–8). As shown in Fig. 4A, the myotube twitched almost concurrently with every light or electric pulse at frequencies between 1 and 4 Hz. However, the response to 5 Hz stimulation varied from one myotube to another. In the case shown in Fig. 4A, the contraction was attenuated by light or electric pulses given in the later period (Supplementary Movie S9, 10). Otherwise, the myotube twitched robustly at 5 Hz (Fig. 4B and Supplementary Movie S11, 12) or exhibited tetanus-like sustained contraction (Fig. 4C and Supplementary Movie S13, 14) during either optical or electrical stimulation. The optically evoked contractions were almost similar to the electrically evoked ones in both the contractile pattern and the magnitude as indicated by the average contraction lengths during the stimulation period (Fig. 4D). Therefore, the various contractile patterns at high-frequency stimulation could be attributed to the various maturational levels of the myotubes. In some myotubes, the optical stimulation evoked no contractions at the maximal light intensity, probably because of the low expression level of ChR2.

Muscle fibers in vivo have been subjected contractile activity under the regulation of nerve-muscle synapses. However, it has been difficult to engineer neuro-muscular synapses in vitro to manipulate microdevices with desired accuracy. Hitherto, electrical field stimulation has been mainly used for artificial contraction of skeletal muscles. However, it has several disadvantages such as low point-to-point discrimination, electrolysis of electrodes, and tissue damage. In contrast, optical methods allow one to stimulate muscle cells without any contact with tissue or extracellular fluid, and thus are non-invasive in principle. Since the optical signal is also high in both spatial and temporal resolutions, it should enable one to control the muscle contraction accurately with given spatial and temporal patterns, which has never been achieved by electrical stimulation.

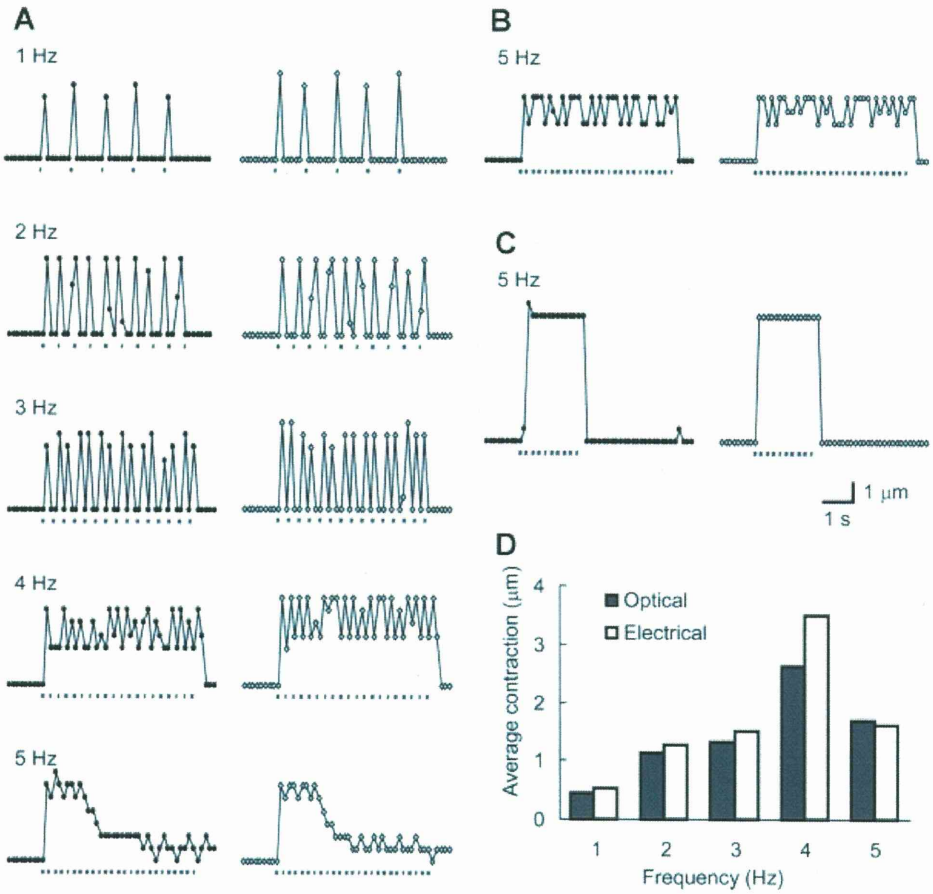

Figure 4. Optically evoked contraction of ChR2-expressing C2C12 myotube. **A**: Typical contraction patterns of a myotube during a 5-s train of LED pulses (0.12 mW/mm^2, 100 ms duration) each at 1, 2, 3, 4, and 5 Hz (from top to bottom of the left column) or during electrical field stimulation (0.8 V/mm, 100 ms duration, right column). **B**: Pulse-to-pulse contraction of another myotube at 5 Hz. **C**: An example of tetanus-like contraction evoked by 5 Hz photostimulation. **D**: Average contraction length during the stimulation period of 5 s of a ChR2-expressing myotube in response to either optical or electrical field stimuli. From the same myotube shown in A. The same scales for A–C.

Conclusions

In this paper it was shown that the C2C12 myotubes became photosensitive by the expression of one of the light-gated channels, ChR2, and that optical stimulation using LED light pulses was able to control their contractile activity with a given temporal pattern. This technique would have many potential bioengineering applications such as wireless drive of muscle-powered actuators/microdevices and aneural culture model systems that may be used for the study of muscle fiber maturation, muscle bioassays for biological and mechanical properties, and pathophysiological study of muscular dystrophy. With the development of ES/iPS-cell technologies, the present methods would enable one to generate human muscle tissue substitutes the contraction of which is optically regulated.

The authors are grateful to K. Nagamine and M. Kanzaki for technical advices and to B. Bell and D. Teh for language assistance. This work was supported by grant-in-aid for Japan Society for the Promotion of Science (JSPS) Fellows, Core Research for Evolutional Science and Technology (CREST), Japan Science and Technology Agency (JST) and grants-in-aid for scientific research from the Ministry of Education, Culture, Sports, Science and Technology (MEXT) of Japan.

References

Bers DM. 2002. Cardiac excitation-contraction coupling. Nature 415(6868): 198–205.

Blau HM, Chiu C-P, Webster C. 1983. Cytoplasmic activation of human nuclear genes in stable heterocaryons. Cell 32(4):1171–1180.

Boyden ES, Zhang F, Bamberg E, Nagel G, Deisseroth K. 2005. Millisecond-timescale, genetically targeted optical control of neural activity. Nat Neurosci 8(9):1263–1268.

Callaway EM, Yuste R. 2002. Stimulating neurons with light. Curr Opin Neurobiol 12(5):587–592.

Engler AJ, Griffin MA, Sen S, Bonnetnann CG, Sweeney HL, Discher DE. 2004. Myotubes differentiate optimally on substrates with tissue-like stiffness: Pathological implications for soft or stiff microenvironments. J Cell Biol 166(6):877–887.

Feinberg AW, Feigel A, Shevkoplyas SS, Sheehy S, Whitesides GM, Parker KK. 2007. Muscular thin films for building actuators and powering devices. Science 317(5843):1366–1370.

Fujita H, Nedachi T, Kanzaki M. 2007. Accelerated de novo sarcomere assembly by electric pulse stimulation in C2C12 myotubes. Exp Cell Res 313(9):1853–1865.

Ishizuka T, Kakuda M, Araki R, Yawo H. 2006. Kinetic evaluation of photosensitivity in genetically engineered neurons expressing green algae light-gated channels. Neurosci Res 54(2):85–94.

Kaji H, Ishibashi T, Nagamine K, Kanzaki M, Nishizawa M. 2010. Electrically induced contraction of C2C12 myotubes cultured on a porous membrane-based substrate with muscle tissue-like stiffness. Biomaterials 31(27):6981–6986.

Kamada M, Li RY, Hashimoto M, Kakuda M, Okada H, Koyanagi Y, Ishizuka T, Yawo H. 2004. Intrinsic and spontaneous neurogenesis in the postnatal slice culture of rat hippocampus. Eur J Neurosci 20(10): 2499–2508.

Kim J, Park J, Yang S, Baek J, Kim B, Lee SH, Yoon E-S, Chun K, Park S. 2007. Establishment of a fabrication method for a long-term actuated hybrid cell robot. Lab Chip 7(11):1504–1508.

Li X, Gutierrez DV, Hanson MG, Han J, Mark MD, Chiel H, Hegemann P, Landmesser LT, Herlitze S. 2005. Fast noninvasive activation and inhibition of neural and network activity by vertebrate rhodopsin and green algae channelrhodopsin. Proc Natl Acad Sci USA 102(49): 17816–17821.

Miesenböck G. 2004. Genetic methods for illuminating the function of neural circuits. Curr Opin Neurobiol 14(3):395–402.

Morishima K, Tanaka Y, Ebara M, Shimizu T, Kikuchi A, Yamato M, Okano T, Kitamori T. 2006. Demonstration of a bio-microactuator powered by cultured cardiomyocytes coupled to hydrogel micropillars. Sens Act B Chem 119(1):345–350.

Nagai T, Ibata K, Park ES, Kubota M, Mikoshiba K, Miyawaki A. 2002. A variant of yellow fluorescent protein with fast and efficient maturation for cell-biological applications. Nat Biotechnol 20(1):87–90.

Nagamine K, Kawashima T, Ishibashi T, Kaji H, Kanzaki M, Nishizawa M. 2010. Micropatterning contractile C2C12 myotubes embedded in a fibrin gel. Biotechnol Bioeng 105(6):1161–1167.

Nagamine K, Kawashima T, Sekine S, Ido Y, Kanzaki M, Nishizawa M. 2011. Spatiotemporally controlled contraction of micropatterned skeletal muscle cells on a hydrogel sheet. Lab Chip 11(3):513–517.

Nagel G, Szellas T, Huhn W, Kateriya S, Adeishvili N, Berthold P, Ollig D, Hegemann P, Bamberg E. 2003. Channelrhodopsin-2, a directly light-gated cation-selective membrane channel. Proc Natl Acad Sci USA 100(24):13940–13945.

Nakanishi K, Dohmae N, Morishima N. 2007. Endoplasmic reticulum stress increases myofiber formation in vitro. FASEB J 21(11):2994–3003.

Nedachi T, Kanzaki M. 2006. Regulation of glucose transporters by insulin and extracellular glucose in C2C12 myotubes. Am J Physiol Endocrinol Metab 291(4):E817–828.

Tanaka Y, Sato K, Shimizu T, Yamato M, Okano T, Kitamori T. 2007. A micro-spherical heart pump powered by cultured cardiomyocytes. Lab Chip 7(2):207–212.

Wilson K, Das M, Wahl KJ, Colton RJ, Hickman J. 2010. Measurement of contractile stress generated by cultured rat muscle on silicon cantilevers for toxin detection and muscle performance enhancement. Plos One 5(6):e11042.

Xi J, Schmidt JJ, Montemagno CD. 2005. Self-assembled microdevices driven by muscle. Nat Mater 4(2):180–184.

Yaffe D, Saxel ORA. 1977. Serial passaging and differentiation of myogenic cells isolated from dystrophic mouse muscle. Nature 270(5639):725–727.

Yamaguchi T, Suzuki T, Arai H, Tanabe S, Atomi Y. 2010. Continuous mild heat stress induces differentiation of mammalian myoblasts, shifting fiber type from fast to slow. Am J Physiol Cell Physiol 298(1):C140–C148.

Yamasaki K, Hayashi H, Nishiyama K, Kobayashi H, Uto S, Kondo H, Hashimoto S, Fujisato T. 2009. Control of myotube contraction using electrical pulse stimulation for bio-actuator. J Artif Organs 12(2):131–137.

OPEN ACCESS Freely available online

PLoS one

Light-evoked Somatosensory Perception of Transgenic Rats That Express Channelrhodopsin-2 in Dorsal Root Ganglion Cells

Zhi-Gang Ji[1,2], Shin Ito[1,2], Tatsuya Honjoh[1,2], Hiroyuki Ohta[1,3], Toru Ishizuka[1], Yugo Fukazawa[4], Hiromu Yawo[1,2,5]*

1 Department of Developmental Biology and Neuroscience, Tohoku University Graduate School of Life Sciences and JST, CREST, Sendai, Japan, **2** Tohoku University Basic and Translational Research Centre for Global Brain Science, Sendai, Japan, **3** Department of Physiology, National Defense Medical College, Tokorozawa, Japan, **4** Department of Anatomy and Molecular Cell Biology, Nagoya University Graduate School of Medicine, Nagoya, Japan, **5** Center for Neuroscience, Tohoku University Graduate School of Medicine, Sendai, Japan

Abstract

In vertebrate somatosensory systems, each mode of touch-pressure, temperature or pain is sensed by sensory endings of different dorsal root ganglion (DRG) neurons, which conducted to the specific cortical loci as nerve impulses. Therefore, direct electrical stimulation of the peripheral nerve endings causes an erroneous sensation to be conducted by the nerve. We have recently generated several transgenic lines of rat in which channelrhodopsin-2 (ChR2) transgene is driven by the Thy-1.2 promoter. In one of them, W-TChR2V4, some neurons were endowed with photosensitivity by the introduction of the ChR2 gene, coding an algal photoreceptor molecule. The DRG neurons expressing ChR2 were immunohistochemically identified using specific antibodies to the markers of mechanoreceptive or nociceptive neurons. Their peripheral nerve endings in the plantar skin as well as the central endings in the spinal cord were also examined. We identified that ChR2 is expressed in a certain population of large neurons in the DRG of W-TChR2V4. On the basis of their morphology and molecular markers, these neurons were classified as mechanoreceptive but not nociceptive. ChR2 was also distributed in their peripheral sensory nerve endings, some of which were closely associated with CK20-positive cells to form Merkel cell-neurite complexes or with S-100-positive cells to form structures like Meissner's corpuscles. These nerve endings are thus suggested to be involved in the sensing of touch. Each W-TChR2V4 rat showed a sensory-evoked behavior in response to blue LED flashes on the plantar skin. It is thus suggested that each rat acquired an unusual sensory modality of sensing blue light through the skin as touch-pressure. This light-evoked somatosensory perception should facilitate study of how the complex tactile sense emerges in the brain.

Citation: Ji Z-G, Ito S, Honjoh T, Ohta H, Ishizuka T, et al. (2012) Light-evoked Somatosensory Perception of Transgenic Rats That Express Channelrhodopsin-2 in Dorsal Root Ganglion Cells. PLoS ONE 7(3): e32699. doi:10.1371/journal.pone.0032699

Editor: Mark L. Baccei, University of Cincinnatti, United States of America

Received October 18, 2011; **Accepted** January 29, 2012; **Published** March 6, 2012

Funding: Funding was provided by the Program for Promotion of Fundamental Studies in Health Sciences of the National Institute of Biomedical Innovation (NIBIO), Japan; Global COE Program (Basic & Translational Research Centre for Global Brain Science), MEXT (Ministry of Education, Culture, Sports, Science, and Technology), Japan; and Strategic Research Program for Brain Sciences (SRPBS), MEXT, Japan. The funders had no role in study design, data collection and analysis, decision to publish, or preparation of the manuscript.

Competing Interests: The authors have declared that no competing interests exist.

* E-mail: yawo-hiromu@m.tohoku.ac.jp

Introduction

Knowledge of the world is obtained exclusively via perception through our sensory systems which consist of peripheral sensory organs, sensory nerves and the central nervous system (CNS). In principle, a sensation is classified according to its modality, that is, the kind of energy inducing physiological transduction in a specific group of sensory organs. For example, in the somatosensory systems, each mode of touch-pressure, temperature or pain is sensed by sensory endings of different dorsal root ganglion (DRG) neurons. Their signals are conducted to a specific cortical locus as nerve impulses, which are then integrated to generate somatosensory perception. Therefore, non-physiological energy transduction such as direct electrical stimulation of a peripheral nerve causes an erroneous sensation to be conducted by the nerve.

In the case of light, rhodopsins are molecules involved in its perception by the photoreceptor cells in the vertebrate retina [1,2]. Each rhodopsin is a seven-pass transmembrane molecule, homologous to G-protein-coupled receptors, and activates cyclic GMP phosphodiesterase upon activation. With the subsequent reduction of the intracellular level of cGMP, the cyclic-nucleotide-gated cation channels are closed [3,4]. A light signal is thus converted into an electrical one through a cascade of at least four molecules. On the other hand, light is perceived by archaea-type rhodopsins, channelrhodopsin-1 (ChR1) and -2 (ChR2), during the light-directed behavior of a unicellular green alga, *Chlamydomonas reinhardtii* [5–9]. Each channelrhodopsin consists of a seven-pass transmembrane apoprotein and a retinal which covalently binds to it. The photoisomerization of all-*trans*-retinal to the 13-*cis* configuration is coupled to conformational changes in the protein that result in increased cation permeability. A light signal is thus converted into an electrical one by a single molecule [10]. Previously, it was reported that neurons were endowed with sensitivity to blue light by introduction of the ChR2 gene [11–13].

This optogenetic method has become a powerful tool for the investigation of neural networks in various animals. It also has potential as a visual prosthesis in case of photoreceptor degeneration [14–16].

Different modalities, such as pain, temperature and touch, are mixed when an animal senses the world through its skin. However, by the selective expression of ChR2 in a subset of nociceptive DRG neurons, the modality-specific circuitry has been optically investigated [17,18]. We have recently generated several transgenic rat lines in which ChR2 transgene is driven by the Thy-1.2 promoter [16]. In one of these lines, W-TChR2V4, some neurons were endowed with photosensitivity by this introduction of ChR2; specifically, these neurons were the retinal ganglion cells, the principal neurons in the cerebral cortex and hippocampus, as well as other brain regions. (Figure S1). In this study, we identified that ChR2 is expressed in a certain population of large neurons in the DRG of a rat from this line. On the basis of their morphology and molecular markers, these neurons were classified as mechanoreceptive but not nociceptive. ChR2 was also found to be distributed in their peripheral sensory nerve endings. As the blue light evoked sensory nerve responses through the skin, it appeared to induce the sense of touch in the rats. It is thus suggested that the sensory modality of the somatosensory system was modified to induce reactivity to blue light in these transgenic rats.

Results

ChR2 expression in DRG

The distribution of ChR2-*Venus* conjugates (ChR2V) was immunohistochemically identified using the W-TChR2V4 line. As shown in Figure 1A, the ChR2V-expressing (ChR2V+) DRG neurons always co-expressed NF200 (111/111 neurons, 100%, Figure 1E), one of the markers of myelinated neurons. On the other hand, almost negligible numbers of the ChR2V+ DRG neurons were positive for calcitonin gene-related peptide (CGRP) (3/279 neurons, 1.1%, Figure 1E) (Figure 1B) or $P2X_3$ (7/161 neurons, 4.3%, Figure 1E) (Figure 1C). Previous studies have shown that some of the myelinated A fibers are also involved in proprioception [19,20]. Parvalbumin (PV), a member of the family of low-molecular-weight calcium-binding proteins, has been shown to be preferentially expressed within large DRG neurons and is considered to be a highly specific molecular marker for primary proprioceptors [21,22]. As shown in Figure 1D, some of the ChR2V+ DRG neurons co-expressed PV (108/253 neurons, 43%, Figure 1E). Although not all NF200-positive neurons were ChR2V+ (111/236, 47%), most of the PV-positive neurons were ChR2V+ (108/115 neurons, 94%) (Figure 1F).

The size of each DRG neuron was evaluated by its average diameter, as summarized in Figure 2. The ChR2V+ DRG neurons (diameter, 43 ± 0.42 μm, $n = 212$) were clearly discriminated in terms of size from the CGRP-positive DRG neurons (diameter, 23 ± 0.34 μm, $n = 230$), with a statistically significant difference ($P \ll 10^{-10}$, two-tailed *t*-test). Their size distribution was also different from that of the $P2X_3$-positive DRG neurons (diameter, 23 ± 0.24 μm, $n = 229$; $P \ll 10^{-10}$, two-tailed *t*-test), although three $P2X_3$-positive neurons had diameters between 35 and 45 μm. On the other hand, there was no significant difference in size between the CGRP- and the $P2X_3$-positive groups. The NF200-positive neurons ($n = 236$) appeared to consist of at least two groups, one with diameters smaller than 30 μm and the other with diameters larger than 30 μm. The ChR2V+ DRG neurons were segregated from the former group but co-localized with the latter.

ChR2 expression in dorsal spinal cord

In the dorsal spinal cord, the gray matter has been anatomically classified into five discrete layers [23]. As shown in Figure 3A–C, the ChR2V was broadly distributed in the spinal cord gray matter (see also Figure S2). However, it was negligible in the outer dorsal layers where CGRP immunoreactivity was present (Figure 3B). Similarly, the ChR2V was not co-localized with $P2X_3$ immunoreactivity in the inner dorsal layers (Figure 3C). On the other hand, the distribution of ChR2V overlapped with that of NF200 immunoreactivity (Figure 3A).

ChR2 expression in the peripheral nerve endings

As previously noted, ChR2 was expressed in large DRG neurons, which have been suggested to be involved in proprioception and touch-pressure sensing. The above results showed that only a subpopulation of ChR2V+ DRG neurons co-expressed PV, a marker of proprioceptive neurons. Therefore, it is probable that another subpopulation of these neurons have myelinated nerves involved in touch-pressure, which project their peripheral endings to the skin as mechanoreceptors. In the superficial layer of the skin, indeed, the ChR2V+ nerve bundles were also positive for myelin basic protein (MBP), which is a marker of myelinated axons (Figure 4A). Some of the peripheral endings of mechanoreceptive neurons have been shown to be associated with Merkel cells, which specifically express cytokeratin-20 (CK20), and form Merkel corpuscles in the skin [24], or with lamellar cells of Meissner's corpuscles, which express S-100 [25]. As shown in Figures 4B and 4C, ChR2V+ nerve endings were frequently associated with CK20-positive Merkel cells or with S-100-positive cells to form structures morphologically reminiscent of Meissner's corpuscles. On the other hand, they were not co-localized with the CGRP-positive free nerve endings assumed to be involved in nociception (Figure 4D). Peripherally, some of the proprioceptive DRG neurons projected to the intrafusal muscles as sensory spiral endings. As shown in Figure 4E, ChR2V+ nerve endings were frequently found in muscle. Some of them were motor nerve terminals as the spinal motor neurons also expressed ChR2V (Figure S2). Others were found in the muscle spindles with spiral appearances and co-expressed PV (Figure 4E).

Sensitivity to blue light

We next evaluated the sensitivity of ChR2V+ DRG neurons to blue light. For this evaluation, the DRG neurons were cultured and the ChR2V expression was identified by the presence of *Venus* fluorescence. Under whole-cell voltage clamp, blue LED light pulse evoked a photocurrent in every ChR2V+ neuron (24/24 neurons) (Figure 5A). Both the peak and the steady-state photocurrents were dependent on the light power density (Figure 5B). The peak current ranged between -0.5 and -5.2 nA ($n = 24$) at the maximal irradiance, although unclamped currents from escaped action potentials were frequently observed. Under the current clamp, the blue LED light pulse (200 ms) evoked rapid membrane depolarization in an intensity-dependent manner and, eventually, only one action potential in 16 of 18 experiments (Figure 5C). In the remaining two cases, the blue LED light evoked subthreshold depolarization even at the maximum irradiance. The size of the action potential varied from cell to cell (range, 15–72 mV, $n = 16$) with threshold irradiances of 0.06–1.3 $mWmm^{-2}$ (Figure 5D). However, the same blue LED light did not evoke any current or voltage response in the ChR2V-negative (ChR2V−) DRG neurons ($n = 3$, Figure S3).

When short LED pulses (duration, 20 ms) were repeatedly applied at the maximal irradiance (1.6 $mWmm^{-2}$), they robustly evoked action potentials at low frequency (Figures 5E and 5F). For

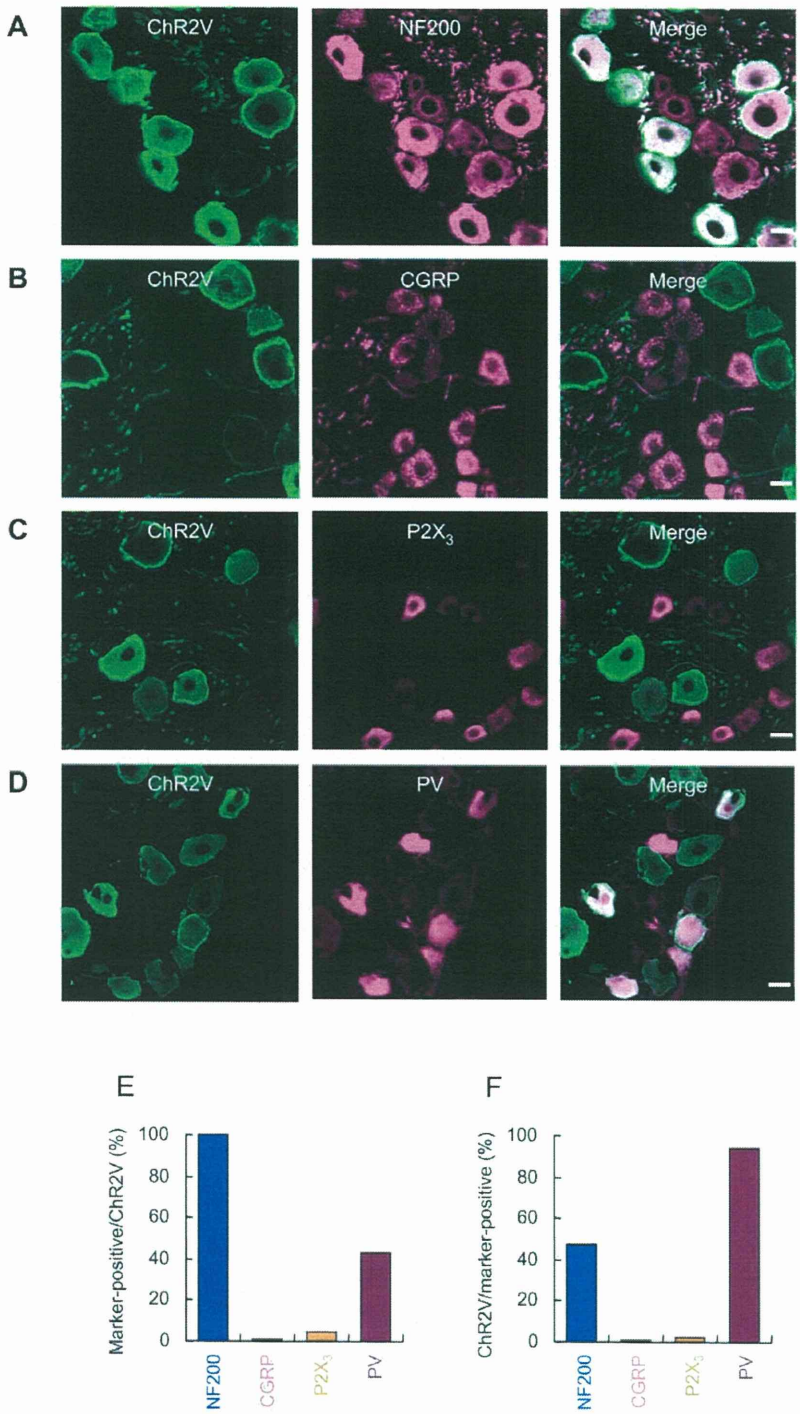

Figure 1. Distribution of channelrhodopsin 2-*Venus* conjugates (ChR2V) in the dorsal root ganglion (DRG) of W-TChR2V4 rats. A–D. Immunohistochemical identification of ChR2V-expressing neurons using cell-type specific markers, NF200 (A), CGRP (B), $P2X_3$ (C) and PV (D). Scale bars indicate 20 μm. E. Probability of the co-expression of each marker, NF200, CGRP, $P2X_3$ or PV, in the ChR2V+ neurons. F. Probability of the co-expression of ChR2V in the neurons positive for each marker, NF200, CGRP, $P2X_3$ or PV.
doi:10.1371/journal.pone.0032699.g001

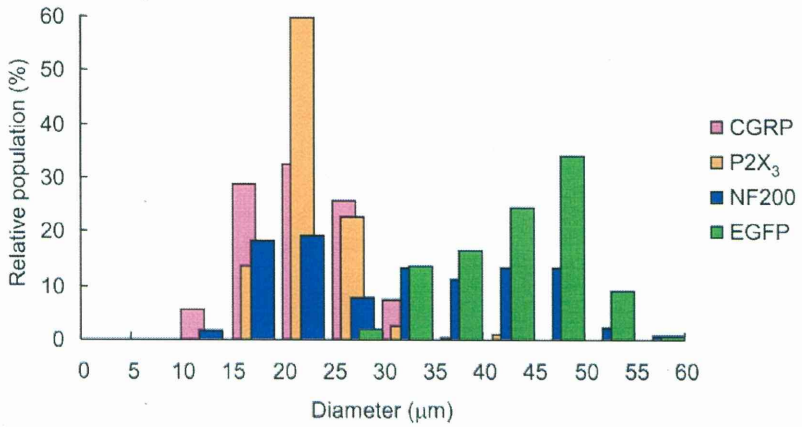

Figure 2. The average diameters of DRG neurons were compared among four groups positive for ChR2V (green), NF200 (blue), CGRP (magenta) and $P2X_3$ (orange).
doi:10.1371/journal.pone.0032699.g002

example, there was no failure of the action potential in 13/14 neurons at 1 Hz, 12/14 at 2 Hz and 10/14 at 5 Hz. However, the fidelity was reduced at increased frequencies: 6/14 at 10 Hz and 3/14 at 20 Hz.

Behavioral responses to light

On the basis of the above evidence, we could expect that the blue light on the plantar skin evokes tactile perception in this transgenic rat. To test this, hindpaws of rats were illuminated at the plantar skin by a series of blue or red LED flashes (duration, 50 ms; 10 pulses at 10 Hz; interval, 10 s) while the rest of the body was shaded with a black cloth (Figure 6A). Although the rats remained quiet, the ChR2V+ rats appeared to move the paw in response to the blue LED flash on its plantar skin (Video S1). The

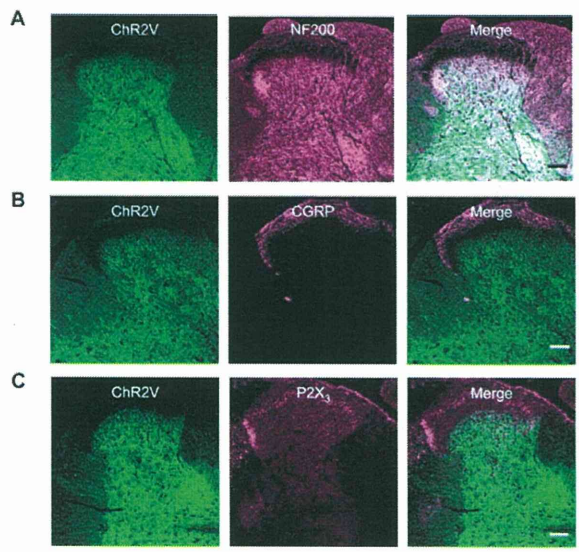

Figure 3. Distribution of ChR2V in the dorsal part of the spinal cord. A–C. Immunohistochemical localization of ChR2V with the cell-type specific markers, NF200 (A), CGRP (B) or $P2X_3$ (C). Scale bars indicate 40 μm.
doi:10.1371/journal.pone.0032699.g003

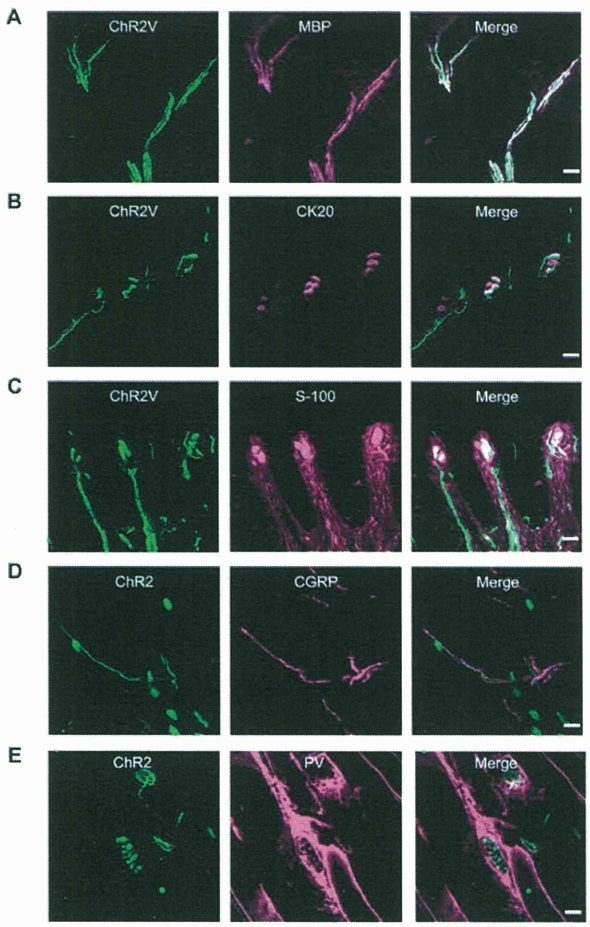

Figure 4. Distribution of ChR2V in the peripheral sensory nerve endings. A–D. Immunohistochemical identification of the ChR2V+ nerve endings in the skin in relation to MBP (A), CK20 (B), S-100 (C) or CGRP (D). E. Co-localization of the ChR2V+ nerve endings with PV in the muscle spindle. Scale bars indicate 20 μm.
doi:10.1371/journal.pone.0032699.g004

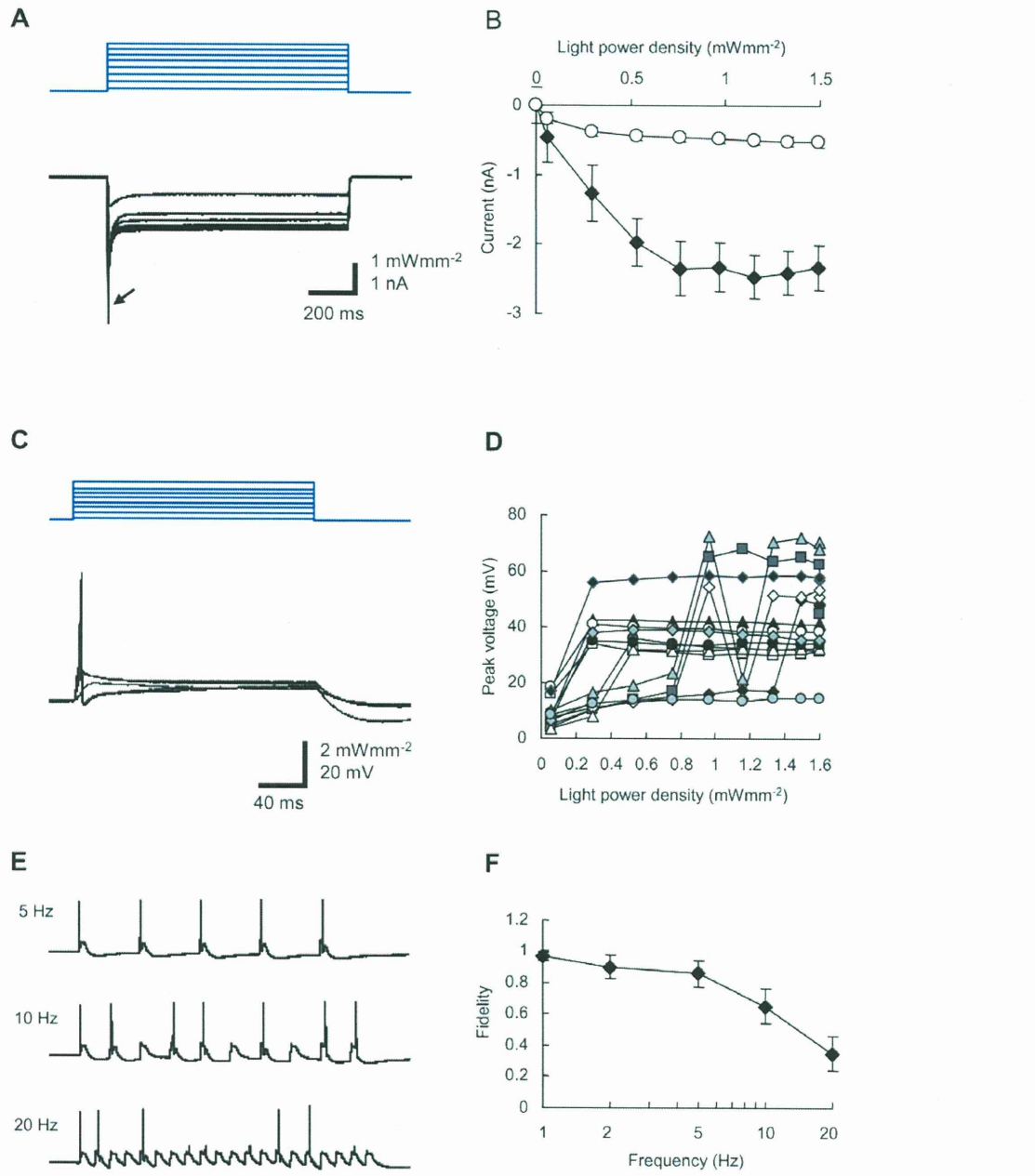

Figure 5. Optical responses of the ChR2V+ DRG neurons. A. Representative records of photocurrents (bottom) evoked by blue LED light of variable strength (top) under voltage clamp. An arrow indicates the unclamped current from escaped action potentials. B. The peak (closed diamonds) and the steady-state (open squares) photocurrent amplitudes (mean ± SEM, both n = 24) as functions of the light power density. C. Representative records of the neuronal membrane potential evoked by blue LED pulses (200 ms) of variable strength under current clamp. The resting membrane potential, −56 mV. D. The maximal voltage changes as a function of the light power density (n = 16). E. Representative records of membrane potential responses of a ChR2V-expressing DRG neuron to the repeated flashing of blue LED pulses (1.6 mWmm^{-2}, 20 ms duration) at various frequencies, that is, 5 Hz (top), 10 Hz (middle) and 20 Hz (bottom). F. Fidelity of generation of action potentials as a function of frequency (mean ± SEM, n = 14).
doi:10.1371/journal.pone.0032699.g005

blue LED flashes clearly and robustly evoked reflexive movements of the paw or toe, whereas the red LED flashes did not (Video S2). The movements during flashing exposure were scored according to their magnitudes (Table 1). The proportion of cases when movement occurred during flashing with blue light was 100%, whereas it was 25±68% with red light, showing a significant difference ($P<0.05$, Wilcoxon signed-rank test, n = 8 animals). Relatively large movements (score, 2–3) were frequently evoked by the blue LED flashes (Figure 6B). There was a significant difference between blue and red flashes (n = 8, $P<0.01$, Wilcoxon

signed-rank test) when we compared the average scores given for the magnitude of movement (Figure 6C). As a control, neither blue nor red flashes evoked clear movements in the case of ChR2V− rats (n = 8). Compared with the ChR2V+ rats, the probability of showing large movements (score 2–3) and the average movement scores of the control rats were negligible (Figures 6B and 6C, $P<0.005$, Mann-Whitney *U*-Test). Similarly, the ChR2V+ rats moved their forepaws significantly more frequently and vigorously during blue LED flash than during red LED flashes (Figures 6D and 6E; Videos S3 and S4). We also tested the light-evoked movement of tails, but only one ChR2V+ rat showed clear responses to the blue LED flashes (Video S5).

Discussion

In this study, we found that ChR2 is expressed in a certain population of large neurons in the DRG of a transgenic rat line, W-TChR2V4, in which the ChR2V transgene was driven by the Thy-1.2 promoter [16]. The ChR2V+ neurons co-expressed NF200, a marker of medium–large neurons involved in mecha-

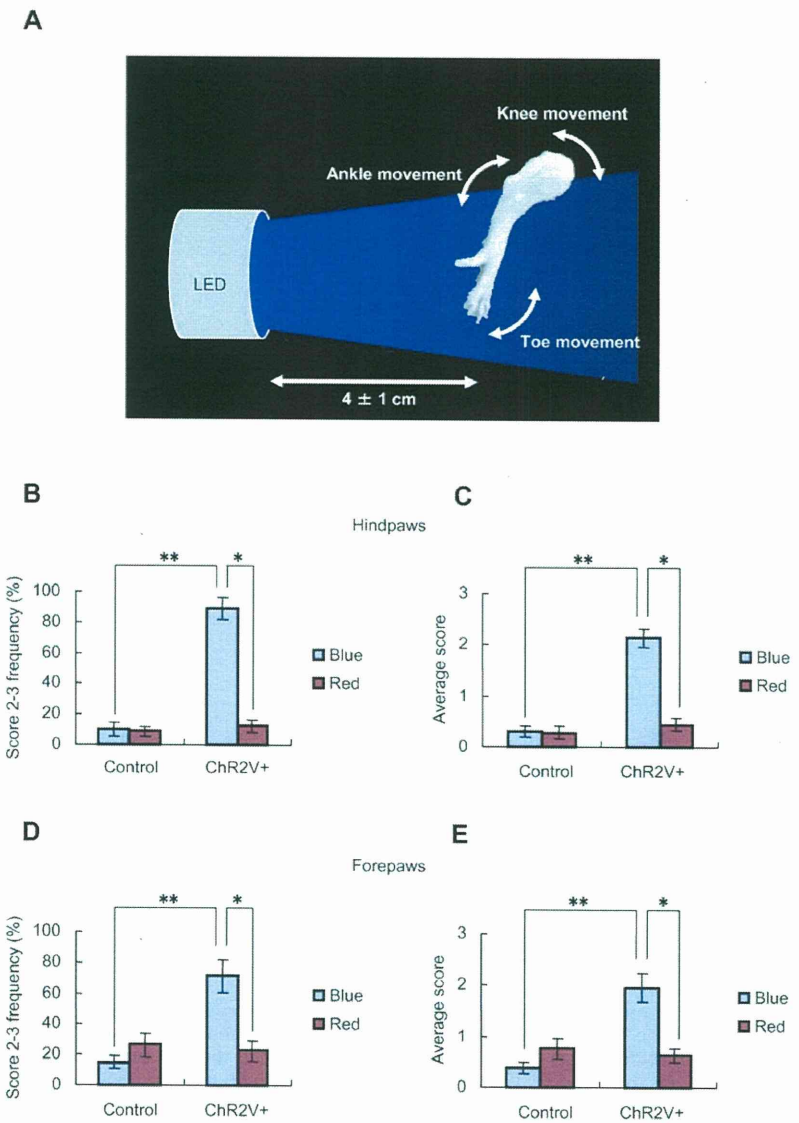

Figure 6. Optically evoked behavioral responses. A. Schematic diagram of the experimental setup. One of four paws was placed in the light path of a blue or red LED so that the plantar skin faced the light while the rest of the body was covered with a black cloth. The distance between the surface of the collimator lens of the LED and the plantar skin was set to about 4 cm, but the exact distance was in the range of 3–5 cm because of the spontaneous movements of the paw. All the experiments were carried out under yellow, dim background light. The optically evoked behavioral responses were scored according to the movement around joints: toe, ankle/wrist or knee/elbow (Table 1). B and C. Light-evoked responses of hindpaws were compared between the wild-type (n = 8) and the ChR2V+ rats (n = 8). The probability of large movements (score 2–3, B) or the average score over ten successive tests (C) was compared between blue and red LED light. D and E. Light-evoked responses of forepaws of the same group of rats: the probability of large movements (score 2–3, D) or the average score (E). Wicoxon signed-rank test was applied for the paired data (*, $P<0.01$) and Mann-Whitney *U*-test for unpaired data (**, $P<0.0005$).
doi:10.1371/journal.pone.0032699.g006

Table 1. The behavioral response score.

Behavior	Score
No response	0
Toe movements	1
Ankle or wrist movements	2
Knee or elbow movements	3

doi:10.1371/journal.pone.0032699.t001

noreception, but not CGRP or $P2X_3$, markers of small neurons involved in nociception. Since the peripheral sensory nerve endings also expressed ChR2, it was expected that photostimulation would evoke action potentials in them. Indeed, the ChR2V+ rats showed sensory-evoked behaviors in response to blue LED flash on their plantar skin. It is thus suggested that the rats had acquired an unusual sensory modality enabling them to sense blue light through the skin.

ChR2V+ DRG neurons are not involved in nociception

The DRG comprises cell bodies of functionally distinct sensory nerves. The DRG neurons have been classified in terms of various characteristics, for example, fast-conducting vs. slow-conducting, myelinated vs. non-myelinated, nociceptive vs. non-nociceptive or small vs. large. In this study, we used NF200 as a marker of myelinated neurons and found that almost all ChR2V+ DRG neurons co-expressed NF200. On the other hand, some NF200-expressing DRG neurons were ChR2V−. It is thus suggested that the ChR2V-expressing DRG neurons are a subpopulation of the fast-conducting myelinated neurons.

The nociceptive neurons can be further classified into peptidergic and non-peptidergic neurons. The peptidergic neurons are immunoreactive to substance P (SP) or CGRP, whereas the non-peptidergic neurons are immunoreactive to isolectin B4 (IB4) or purinergic receptor $P2X_3$ [26–28]. We found that almost all the ChR2V+ neurons were negative for both CGRP and $P2X_3$. Therefore, the nociceptive DRG neurons appeared to be mostly ChR2V−.

In our study over 98% of the ChR2V+ DRG neurons had diameters larger than 30 μm. Although the neuron size is dependent on the age or the body size of the rat, these neurons were classified as medium–large [29–31]. On the other hand, the nociceptive neurons that expressed either CGRP or $P2X_3$ were mostly small. The size distribution of ChR2V+ neurons appeared to be distinct from that of nociceptive neurons. However, a small number of medium-sized DRG neurons were also positive for $P2X_3$. A subpopulation of NF200-expressing DRG neurons were discriminated from ChR2V+ DRG neurons by their small size (diameter<30 μm). It is possible that these DRG neurons were small myelinated Aδ-fiber neurons involved in pain [32]. These observations are consistent with the notion that the ChR2V+ neurons are not involved in nociception [33,34], although further studies are necessary to confirm this.

In the spinal cord, neurons involved in nociception are located in the marginal layer (lamina I) and the substantia gelatinosa (lamina II) of the dorsal horn and receive inputs from the nociceptive DRG neurons [35,36]. Indeed, various noxious stimuli induce acute c-Fos expression in these laminae [37]. On the other hand, the myelinated fibers involved in mechanoreception are projecting predominantly to laminae III–V [35–38]. Consistent with these previous studies, immunoreactivity to CGRP or $P2X_3$ was predominantly present in laminae I and II and that to NF200 was negligible in these superficial layers. We found that the ChR2V expression co-localized with neither with CGRP nor $P2X_3$. It is thus suggested that the ChR2V+ fibers are myelinated and involved in mechanoreception.

We also found in the plantar skin that the ChR2V+ nerve fibers were mostly associated with MBP immunoreactivity. It is thus suggested that these fibers were myelinated and distinct from the nociceptive C-fibers that were unmyelinated. They are also unlikely to be nociceptive Aδ fibers that had lost their myelin before entering the skin [39]. On the other hand, ChR2V-positive nerve endings were frequently associated with Merkel cells in the dermis or with S-100-positive cells to form structures like Meissner's corpuscles, suggesting their involvement in the sense of touch-pressure. However, we did not find the axon terminals in the deep mechanoreceptive structures such as Pacinian corpuscles; this was probably because our histological studies were limited to the superficial layer of the plantar skin. Some of the ChR2V+ fibers appeared to be involved in proprioception since they innervated the muscle spindle to form stretch receptors that were PV-positive.

Taken together, the above histological characteristics suggest that ChR2V was not expressed in most nociceptive DRG neurons. Rather, it appeared to be expressed in a subpopulation of mechanoreceptive neurons with myelinated fibers [40]. Some of the ChR2V+ neurons appeared to be involved in proprioception in muscles, tendons and joints since they were also positive for PV. However, others may have innervated the skin and been involved in the sense of touch-pressure.

Light-evoked somatosensory responses

The above findings that the mechanoreceptive DRG neurons expressed ChR2V in both the soma and peripheral endings raised the possibility that the ChR2V+ rats can sense blue light on their skin as if it were a touch. There is further evidence to support this. First, the ChR2V+ DRG neurons were photosensitive and optically depolarized to evoke action potentials. The action potential was generated at the onset of the light pulse and not thereafter, a trait frequently found in mechanoreceptive DRG neurons [41–45]. Second, the ChR2V+ rats moved their paws in response to the blue LED flashes on the plantar skin, but not in response to the red LED flashes. This behavior was not observable in the control ChR2V− rats. Therefore, the light-evoked behaviors were dependent on both the expression of ChR2 and the wavelength (470±17 nm) that is optimal for the activation of ChR2 [9]. As ChR2V was exclusively expressed in the myelinated nerve endings that were non-nociceptive, the blue light was likely to have induced the sense of touch-pressure in the rats. This blue light-evoked response was not clear in other parts of the body such as the tail. It is possible that fur covering the skin would obstruct the penetration of light. Although ChR2V was expressed in motor neurons and their terminals in our rat model (Figure S2), the sensory nerve endings, which lie in the superficial layer of the skin, are expected to be differentially photostimulated because the blue light cannot penetrate deep into the muscle. It is thus suggested that the sensory modality of the somatosensory system was modified so as to be also reactive to blue light in the ChR2V+ rats.

Conclusions

In this work, we have generated an optogenetic rat model that can be used for the research of the somatosensory system. Using ChR2V+ rats, we can discretely photostimulate the mechanoreceptive nerve endings without any effects on the nociceptive free nerve endings. Combined with electrophysiological as well as neuroimaging methods such as fMRI, our rat model should

facilitate study of how complex tactile perception, such as for texture, size and shape, is generated.

Materials and Methods

Ethics Statement

All animal experiments were approved by the Tohoku University Committee for Animal Experiments (Approval No. 2011LsA-23) and were carried out in accordance with the Guidelines for Animal Experiments and Related Activities of Tohoku University as well as the guiding principles of the Physiological Society of Japan and the National institutes of health (NIH), USA.

Animals

The experiments were carried out using offspring of one of the Thy-1 promotor-ChR2-*Venus* transgenic rat lines, W-TChRV4 with the background of Wistar rats [16] mated with wild-type Wistar rat. The littermates were screened by genomic PCR using the appropriate primers (Figure S4), and were determined to be either transgene-positive (ChR2V+) or -negative (ChR2V−). Alternatively, the tip of the tail was freshly examined under fluorescent microscopy to determine whether *Venus* fluorescence was present in the nerve bundle in the tissue (Figure S5). The number of animals in this study was kept to a minimum and, when necessary, all animals were anesthetized to minimize their suffering. Animals had access to food and water ad libitum and were kept under a 12-hour light-dark cycle.

Immunohistochemistry

ChR2V+ rats (five weeks old) were used for the immunohistochemical experiments. They were anesthetized with a ketamine (50 mg/ml, Daiichi Sankyo Co. Ltd., Tokyo, Japan)-xylazine (xylazine hydrochloride, 10 mg/ml, Sigma-Aldrich, St. Louis, MO, USA) mixture (1 ml/kgBW) and transcardially perfused with phosphate-buffered saline (PBS; pH 7.4), followed by 100 ml of 4% paraformaldehyde (PFA) and 0.2% picric acid in PBS. The lumber region of spinal cords together with DRGs, the intercostals muscles and the pedal skin from one of the paws were removed and post-fixed in 4% PFA overnight at 4°C. After cryoprotection through a graded series of sucrose replacements (10%, 20% and 30% in PBS) at 4°C, each tissue was embedded in OCT Compound (4583, Sakura Finetek, Tokyo, Japan) and stored at −80°C.

The localization and cell type of ChR2V-expressing neurons in the tissue were immunohistochemically investigated using anti-EGFP antibody along with the antibody of one of the cell-type-specific markers. Briefly, each frozen section was cut at 16 μm thickness with a cryostat (CM 3050 S, Leica, Wetzlar, Germany), mounted on poly-L-lysine coated slides (Matsunami Glass Ind. Ltd., Kishiwada, Japan) and left to air-dry for 90 min at room temperature. After washing with PBS, slices were incubated for 1 hr in blocking PBS containing 2.5% goat serum, 0.25% carrageenan and 0.1% Triton X-100 at room temperature. Then, the specimens were reacted overnight at 4°C with the primary antibody: rabbit anti-EGFP (1:2,000) [46]; mouse monoclonal anti-NF200 (1:500, N0142, Sigma-Aldrich); rabbit anti-CGRP (1:2,000, C8198, Sigma-Aldrich); guinea-pig anti-CGRP (1:1000, Progen Biotechnik GmbH, Heidelberg, Germany); guinea-pig anti-$P2X_3$ (1:1,000, GP10108, Neuromics, Edina, MN, USA); mouse anti-PV (1:2,000, P3088, Sigma-Aldrich); chicken anti-MBP (1:500, PA1-10008, Thermo Fisher Scientific K.K., Yokohama, Japan), mouse anti-CK20 (1:20, IT-Ks 20.8, Progen Biotechnik GmbH) and mouse anti-S100 (β-subunit) (1:1000, S2532, Sigma-Aldrich). In some specimens, the *Venus* fluorescence signal could be directly examined without any amplification as previously described [47,48]. After 10-min washing three times, the slices were reacted for 1 hr (room temperature) or overnight (4°C) with the combination of the following secondary antibodies (Molecular Probes products from Life Technologies Co., Carlsbad, CA, USA, except for Dylight-549): Alexa Fluor 488-conjugated donkey anti-rabbit IgG (1:500), Alexa Fluor 546-conjugated donkey anti-mouse IgG (1:500), Alexa Fluor 546-conjugated donkey anti-rabbit IgG (1:500) and Alexa Fluor 633-conjugated goat anti-guinea pig IgG (1:500), and Dylight 549-conjugated goat anti-chicken IgY (Thermo Fisher Scientific K.K., 1:100). After washing three times in PBS, the specimens were mounted with Permafluor (Thermo Fisher Scientific K.K.). Images were digitally captured under conventional confocal laser-scanning microscopy (LSM510META, Carl Zeiss, Oberkochen, Germany) and were corrected for brightness and contrast using LSM Image Browser version 3.2 (Carl Zeiss), Photoshop version 6.0 (Adobe Systems Inc, San Jose, CA, USA) and ImageJ (http://rsbweb.nih.gov/ij/). The diameter of a DRG neuron was microscopically measured as the mean of the shortest and longest diameters.

Culture

The DRG neurons of ChR2V+ rats (3–4 weeks) were cultured according to a method reported previously [49] with some modifications. After decapitation, the DRGs from all available spinal levels were taken out and put into an ice-cold dissecting solution. Each DRG was cleaned of the surrounding connective tissue, cut into small pieces and immersed in an enzymatic solution containing 1.0 mg/ml collagenase II (C6885, Sigma-Aldrich), 0.5 mg/ml trypsin (15090-046, a Gibco product from Life Technologies Co.) and 0.1 mg/ml DNase I (Sigma-Aldrich) for 30–45 min at 37°C. The neurons were washed twice with trituration solution containing 2 mg/ml BSA (A7906, Sigma-Aldrich), resuspended in culture medium containing DMEM (D5030, Sigma-Aldrich) supplemented with 3.7 mg/ml $NaHCO_3$, 1 mg/ml D-glucose, 2 mM L-glutamine (G7513, Sigma-Aldrich), 1% penicillin/streptomycin (P0781, Sigma-Aldrich) and 10% FBS (04-001-1, Biological Industries, Beit-Haemek, Israel), and then plated and cultured at 37°C in a humidified incubator with a 95% air and 5% CO_2 atmosphere. The culture medium was changed every two days. The whole-cell recording experiments were carried out within 4–5 days of plating.

Electrophysiology

ChR2V+ DRG neurons were identified under conventional epi-fluorescence microscopy (BH2-RFC, Olympus Optical Co., Tokyo, Japan) equipped with a 40× water-immersion objective (LUMplanP1/IR40×, Olympus) and a conventional filter cube (excitation, 495 nm; dichroic mirror, 505 nm; barrier filter, 515 nm). Electrophysiological recording was performed at 34±2°C (UTC-1000, Ampere Inc., Tokyo, Japan) under whole-cell patch clamp from the soma using an amplifier (EPC 8, HEKA Elektronik Dr. Schulze GmbH, Germany) and computer software (pCLAMP 9, Molecular Devices, LLC, Sunnyvale, CA). The bath solution was composed of (in mM) 138 NaCl, 3 KCl, 2 $CaCl_2$, 1 $MgCl_2$, 4 NaOH, 10 HEPES, 11 glucose, and was adjusted at pH 7.4 by 1 N HCl. The patch pipette solution was composed of (in mM) 125 K-gluconate, 10 KCl, 0.2 EGTA, 10HEPES, 1 $MgCl_2$, 3 MgATP, 0.3Na_2GTP, 10 Na_2-phosphocreatine and 0.1 leupeptin, and was adjusted at pH 7.2 by 1 N KOH. For the optical actuation of a DRG neuron we used a blue LED (470±25 nm wavelength, LXHL-NB98, Philips Lumileds Lighting Co., San Jose, CA, USA) regulated by a pulse generator (SEN-7203, Nihon Kohden, Tokyo, Japan) and computer software

(pCLAMP 9, Molecular Devices, LLC). The maximal light power density of the LED light was 1.6 $mWmm^{-2}$ at the focus.

Behavioral test

Light-dependent behavior was investigated using eight ChR2V-expressing (ChR2V+) (9–21 weeks) and eight non-expressing (ChR2V−) rats, including three littermates (8–14 weeks) and five wild-type Wistar rats (15 weeks). The whole body of a rat, except for one of the four paws and the tail, was shaded from the light with a black cloth. Either a blue (470±17 nm, LXML-PB01-0023, Philips Lumileds Lighting Co.) or a red LED (627±15 nm, LXML-PD01-0030, Philips Lumileds Lighting Co.) was driven by a pulse generator (SEN-7203, Nihon Kohden, Tokyo, Japan) and a DC voltage/current generator/calibrator (R6243, Advantest, Tokyo, Japan). A series of flashes (duration, 50 ms; 10 pulses at 10 Hz; interval, 10 s) was subjected to the skin at a distance of 3–5 cm while the behavior of the rat was captured using a video camera (PC1249, Canon, Tokyo, Japan). All experiments were carried out under yellow, dim background light. The light power density was directly measured using a thermopile (MIR-100Q, Mitsubishi Oil Chemicals, Tokyo, Japan), and was 3–8 $mWmm^{-2}$ at the skin for both the blue and the red LED lights. Under double-blind conditions, the response to light was scored as described in Table 1.

Supporting Information

Video S1 Typical ChR2V+ transgenic rat showed sensory-evoked behavior of a hindpaw in response to a series of blue LED flashes on the plantar skin as if it had been touched.
(MPG)

Video S2 The same hindpaw showed no specific response to a train of red LED flashes.
(MPG)

Video S3 The same rat also showed sensory-evoked behavior of a forepaw in response to a train of blue LED flashes.
(MPG)

Video S4 The same forepaw showed no specific response to a train of red LED flashes.
(MPG)

Video S5 The same rat also showed clear sensory-evoked movement of its tail in response to a train of blue LED flashes as if it had been touched.
(MPG)

Figure S1 Expression of ChR2V in the brain of W-TChR2V4 rat.
(PDF)

Figure S2 Expression of ChR2V in the spinal cord and the motor nerve terminals.
(PDF)

Figure S3 Non-fluorescent DRG neurons were unresponsive to the blue light.
(PDF)

Figure S4 The primers that were used to differentiate ChR2V+ from ChR2V− rats.
(PDF)

Figure S5 Expression of ChR2V in the tail nerve bundles.
(PDF)

Acknowledgments

We wish to thank G. Nagel for the ChR2 cDNA, A. Miyawaki for the *Venus* cDNA, S. Hososhima, S. Inoue, D. Teh, A. Uchida, S. Watanabe and J. Yokose for experimental assistance, and B. Bell and D. Teh for language assistance.

Author Contributions

Conceived and designed the experiments: Z-GJ HY. Performed the experiments: Z-GJ SI TH HO. Analyzed the data: Z-GJ HY. Contributed reagents/materials/analysis tools: TI YF. Wrote the paper: Z-GJ HY.

References

1. Nathans J (1999) The evolution and physiology of human color vision: insights from molecular genetic studies of visual pigments. Neuron 24: 299–312.
2. Palczewski K (2006) G protein-coupled receptor rhodopsin. Annu Rev Biochem 75: 743–767.
3. Kaupp UB, Seifert R (2002) Cyclic nucleotide-gated ion channels. Physiol Rev 82: 769–824.
4. Bradley J, Reisert J, Frings S (2005) Regulation of cyclic nucleotide-gated channels. Curr Opin Neurobiol 15: 343–349.
5. Sineshchekov OA, Jung KH, Spudich JL (2002) Two rhodopsins mediate phototaxis to low and high intensity light in *Chlamydomonas reinhardtii*. Proc Natl Acad Sci U S A 99: 8689–8694.
6. Suzuki T, Yamasaki K, Fujita S, Oda K, Iseki M, et al. (2003) Archaeal-type rhodopsins in *Chlamydomonas*: model structure and intracellular localization. Biochem Biophys Res Commun 301: 711–717.
7. Kateriya S, Nagel G, Bamberg E, Hegemann P (2004) "Vision" in single-celled Algae. News Physiol, Sci 19: 133–137.
8. Nagel G, Ollig D, Fuhrmann M, Kateriya S, Musti AM, et al. (2002) Channelrhodopsin-1: a light-gated proton channel in green algae. Science 296: 2395–2398.
9. Nagel G, Szellas T, Huhn W, Kateriya S, Adeishvili N, et al. (2003) Channelrhodopsin-2, a directly light-gated cation-selective membrane channel. Proc Natl Acad Sci U S A 100: 13940–13945.
10. Hegemann P (2008) Algal sensory photoreceptors. Annu Rev Plant Biol 59: 167–189.
11. Boyden ES, Zhang F, Bamberg E, Nagel G, Deisseroth K (2005) Millisecond-timescale, genetically targeted optical control of neural activity. Nat Neurosci 8: 1263–1268.
12. Li X, Gutierrez DV, Hanson MG, Han J, Mark MD, et al. (2005) Fast noninvasive activation and inhibition of neural and network activity by vertebrate rhodopsin and green algae channelrhodopsin. Proc Natl Acad Sci U S A 102: 17816–17821.
13. Ishizuka T, Kakuda M, Araki R, Yawo H (2006) Kinetic evaluation of photosensitivity in genetically engineered neurons expressing green algae light-gated channels. Neurosci Res 54: 85–94.
14. Bi A, Cui J, Ma YP, Olshevskaya E, Pu M, et al. (2006) Ectopic expression of a microbial-type rhodopsin restores visual responses in mice with photoreceptor degeneration. Neuron 50: 23–33.
15. Tomita H, Sugano E, Yawo H, Ishizuka T, Isago H, et al. (2007) Restoration of visual response in aged dystrophic RCS rats using AAV-mediated channelopsin-2 gene transfer. Invest Ophthalmol Vis Sci 48: 3821–3826.
16. Tomita H, Sugano E, Fukazawa Y, Isago H, Sugiyama Y, et al. (2009) Visual properties of transgenic rats harboring the channelrhodopsin-2' gene regulated by the Thy-1.2 promoter. PLoS One 4: e7679.
17. Campagnola L, Wang H, Zylka MJ (2008) Fiber-coupled light-emitting diode for localized photostimulation of neurons expressing channelrhodopsin-2. J Neurosci Meth 169: 27–33.
18. Wang H, Zylka MJ (2009) *Mrgprd*-expressing polymodal nociceptive neurons innervate most known classes of substantia gelatinosa neurons. J Neurosci 29: 13202–13209.
19. Lawson SN, Waddell PJ (1991) Soma neurofilament immunoreactivity is related to cell size and fibre conduction velocity in rat primary sensory neurons. J Physiol 435: 41–63.
20. Julius D, Basbaum AI (2001) Molecular mechanisms of nociception. Nature 413: 203–210.
21. Celio MR (1990) Calbindin D-28k and parvalbumin in the rat nervous system. Neuroscience 35: 375–475.
22. Ichikawa H, Deguchi T, Nakago T, Jacobowitz DM, Sugimoto T (1994) Parvalbumin, calretinin and carbonic anhydrase in the trigeminal and spinal primary neurons of the rat. Brain Res 655: 241–245.
23. Basbaum AI, Jessell TM (2000) The perception of pain. In: Kandel ER, Schwartz JH, Jessell TM, eds. Principles of Neural Science Fourth Edition. New York: McGraw-Hill. pp 430–491.

24. Moll I, Roessler M, Brandner JM, Eispert AC, Houdek P, et al. (2005) Human merkel cells-aspects of cell biology, distribution and functions. Eur J Cell Biol 84: 259–271.
25. Kinnman E, Aldskogius H, Johansson O, Wiesenfeld-Hallin Z (1992) Collateral reinnervation and expansive regenerative reinnervation by sensory axons into "foreign" denervated skin: an immunohistochemical study in the rat. Exp Brain Res 91: 61–72.
26. Averill S, Mcmahon SB, Clary DO, Reichardt LF, Priestley JV (1995) Immunocytochemical localization of trkA receptors in chemically identified subgroups of adult rat sensory neurons. Eur J Neurosci 7: 1484–1494.
27. Snider WD, McMahon SB (1998) Tackling pain at the source: new ideas about nociceptors. Neuron 20: 629–632.
28. Zhang X, Bao L (2006) The development and modulation of nociceptive circuitry. Curr Opin Neurobiol 16: 460–466.
29. Ha SO, Yoo HJ, Park SY, Hong HS, Kim DS, et al. (2000) Capsaicin effects on brain-derived neurotrophic factor in rat dorsal root ganglia and spinal cord. Brain Res Mol Brain Res 81: 181–186.
30. Fang X, Djouhri L, McMullan S, Berry C, Waxman SG, et al. (2006) Intense isolectin-B4 binding in rat dorsal root ganglion neurons distinguishes C-fiber nociceptors with broad action potentials and high Nav1.9 expression. J Neurosci 26: 7281–7292.
31. Lu SG, Gold MS (2008) Inflammation-induced increase in evoked calcium transients in subpopulations of rat DRG neurons. Neuroscience 153: 279–288.
32. Dawson LF, Phillips JK, Finch PM, Inglis JJ, Drummond PD (2011) Expression of α_1-adrenoceptors on peripheral nociceptive neurons. Neuroscience 175: 300–314.
33. Vulchanova L, Riedl MS, Shuster SJ, Stone LS, Hargreaves KM, et al. (1998) $P2X_3$ is expressed by DRG neurons that terminate in inner lamina II. Eur J Neurosci 10: 3470–3478.
34. Novakovic SD, Kassotakis LC, Oglesby IB, Smith JA, Eglen RM, et al. (1999) Immunocytochemical localization of P2X3 purinoceptors in sensory neurons in naïve rats and following neuropathic injury. Pain 80: 273–282.
35. Caspary T, Anderson KV (2003) Patterning cell types in the dorsal spinal cord: what the mouse mutants say. Nat Rev Neurosci 4: 289–297.
36. Morris R, Cheunsuang O, Stewart A, Maxwell D (2004) Spinal dorsal horn neurone targets for nociceptive primary afferents: do single neurone morphological characteristics suggest how nociceptive information is processed at the spinal level. Brain Res Brain Res Rev 46: 173–190.
37. Coggeshall RE (2005) Fos, nociception and the dorsal horn. Prog Neurobiol 77: 299–352.
38. Todd AJ (2002) Anatomy of primary afferents and projection neurons in the rat spinal dorsal horn with particular emphasis on substance P and the neurokinin 1 receptor. Exp Physiol 87: 245–249.
39. Provitera V, Nolano M, Pagano A, Caporaso G, Stancanelli A, et al. (2007) Myelinated nerve endings in human skin. Muscle Nerve 35: 767–775.
40. Perry MJ, Lawson SN, Robertson J (1991) Neurofilament immunoractivity in populations of rat primary afferent neurons: a quantitative study of phosphorylated and non-phosphorylated subunits. J Neurocytol 20: 746–758.
41. Melean MJ, Bennett PB, Thomas RM (1988) Subtypes of dorsal root ganglion neurons based on different inward currents as measured by whole-cell voltage clamp. Mol Cell Biochem 80: 95–107.
42. Villière V, McLachlan EM (1996) Electrophysiological properties of neurons in intact rat dorsal root ganglia classified by conduction velocity and action potential duration. J Neurophysiol 76: 1924–1941.
43. Price MP, Lewin GR, McIlwrath SL, Cheng C, Xie J, et al. (2000) The mammalian sodium channel BNC1 is required for normal touch sensation. Nature 407: 1007–1011.
44. Tan ZY, Donnelly DF, LaMotte RH (2006) Effects of a chronic compression of the dorsal root ganglion on voltage-gated Na^+ and K^+ currents in cutaneous afferent neurons. J Neurophysiol 95: 1115–1123.
45. Hu J, Chiang LY, Koch M, Lewin GR (2010) Evidence for a protein tether involved in somatic touch. EMBO J 29: 855–867.
46. Tamamaki N, Nakamura K, Furuta T, Asamoto K, Kaneko T (2000) Neurons in Golgi-stain-like images revealed by GFP-adenovirus infection in vivo. Neurosci Res 38: 231–236.
47. Gong S, Zheng C, Doughty ML, Losos K, Didkovsky N, et al. (2003) A gene expression atlas of the central nervous system based on bacterial artificial chromosomes. Nature 425: 917–925.
48. Torsney C, Anderson RL, Ryce-Paul KA, MacDermott AB (2006) Characterization of sensory neuron subpopulations selectively expressing green fluorescent protein in phosphodiesterase 1C BAC transgenic mice. Mol Pain 2: 17.
49. Hu HZ, Li ZW (1997) Modulation by adenosine of GABA-activated current in rat dorsal root ganglion neurons. J Physiol 501: 67–75.

Development, Growth & Differentiation
The Japanese Society of Developmental Biologists
Develop. Growth Differ. (2011) **53**, 357–365
doi: 10.1111/j.1440-169X.2010.01235.x

Original Article

Differentiation of neuronal cells from NIH/3T3 fibroblasts under defined conditions

Zhuo Wang, Eriko Sugano, Hitomi Isago, Teru Hiroi, Makoto Tamai and Hiroshi Tomita*

Tohoku University Institute for International Advanced Interdisciplinary Research, 4-1 Seiryo-machi, Aoba-ku, Sendai 980-8575, Japan

We attempted to test whether the differentiated NIH/3T3 fibroblasts could be differentiated into neuronal cells without any epigenetic modification. First, a neurosphere assay was carried out, and we successfully generated neurosphere-like cells by floating cultures of NIH/3T3 fibroblasts in neural stem cell medium. These spheres have the ability to form sub-spheres after three passages, and express the neural progenitor markers Nestin, Sox2, Pax6, and Musashi-1. Second, after shifting to a differentiating medium and culturing for an additional 8 days, cells in these spheres expressed the neuronal markers β-tubulin and neurofilament 200 and the astrocytic marker glial fibrillary acidic protein (GFAP). Finally, after treating the spheres with all-trans retinoic acid and taurine, the expression of β-tubulin was increased and the staining of photoreceptor markers rhodopsin and recoverin was observed. The present study shows that NIH/3T3 fibroblasts can generate neurosphere-like, neuron-like, and even photoreceptor-like cells under defined conditions, suggesting that the differentiated non-neuronal cells NIH/3T3 fibroblasts, but not pluripotent cells such as embryonic stem cells or induced pluripotent stem cells, may have the potential to be transdifferentiated into neuronal cells without adding any epigenetic modifier. This transdifferentiation may be due to the possible neural progenitor potential of NIH/3T3 fibroblasts that remains dormant under normal conditions.

Key words: differentiation, neural progenitors, neuron, retinoic acid, taurine.

Introduction

Because of their ability to proliferate infinitely and differentiate into cells of all three germ layers, embryonic stem (ES) cells are regarded as superior potential donor cells for cell replacement to treat many diseases (Hoffman & Carpenter 2005; Takahashi & Yamanaka 2006), such as retinitis pigmentosa and age-related macular degeneration, which are typically characterized by the death of photoreceptors (Osakada *et al.* 2008). Photoreceptor replacement in the form of a cell-based therapeutic approach may aid in the restoration of vision.

Zhao *et al.* (2002) demonstrated that ES cell-derived neural progenitors expressed regulatory factors needed for retinal differentiation, and that a small subset of these cells differentiated along the photoreceptor lineage in response to retina-specific epigenetic cues. Ikeda *et al.* (2005) and Osakada *et al.* (2008) generated putative photoreceptors and RPE cells from rodent and primate ES cells by induction with defined factors.

However, in clinical application, the use of ES cells involves ethical problems and immune rejection. Jin *et al.* (2009) demonstrated partial mesenchymal stem cells obtained from umbilical cord blood were able to be differentiated into neuron-like cells or rhodopsin-positive cells *in vitro*. Recently, retinal cells have been generated from mouse- and human-induced pluripotent stem (iPS) cells by introducing four specific factors Oct3/4, Sox2, Klf4, and c-Myc (Takahashi & Yamanaka 2006; Hirami *et al.* 2009; Osakada *et al.* 2009).

Even though the generation and application of iPS cells made it possible to treat patients with their own cell-derived retinal cells, which may resolve the problem of immune rejection, some questions still remain. For example, the introduction of viral vectors and oncogenes c-Myc and Klf4 into the somatic genome limits the utility of iPS cells for patient-specific therapy

*Author to whom all correspondence should be addressed.
Email: hiroshi-tomita@iiare.tohoku.ac.jp
Received 28 June 2010; revised 30 November 2010; accepted 30 November 2010.

(Yamanaka 2007, 2009; Zhou *et al.* 2009). Furthermore, the generation of an iPS cell line takes considerable time (approximately 6 months) and is labor intensive so it can not be generated rapidly (Holden & Vogel 2008).

In the previous studies, most investigators have used undifferentiated cells, such as ES cells, ES cell-derived neural progenitors, bone marrow stromal cells, or iPS cells, as the cell source (Sanchez-Ramos *et al.* 2000; Woodbury *et al.* 2000; Zhao *et al.* 2002; Ikeda *et al.* 2005; Klassen & Reubinoff 2008; Osakada *et al.* 2008; Jin *et al.* 2009). Zhang *et al.* (2010) showed that NIH/3T3 fibroblasts, which are already committed to a specific differentiation destiny, were able to be induced to express neuronal markers, but these cells have to be reprogrammed by adding epigenetic modifiers to make epigenetic modification.

NIH/3T3 fibroblasts, derived from an embryo of the NIH/Swiss mouse, are generally adherently cultured in Dulbecco's modified Eagle's medium (DMEM) supplemented with 10% bovine calf serum, which is the normal culture condition for most investigators. In the present study, we cultured NIH/3T3 cells in a completely different microenvironment to establish whether this cell line could be induced into neuronal cells without adding any epigenetic modifier and to be further induced into retinal photoreceptor-like cells simply by adding taurine and retinoic acid (RA), and we also characterized the mechanism involved.

Materials and methods

Culture of NIH/3T3 fibroblasts

NIH/3T3 fibroblasts were kindly provided by the Cell Resource Center for Biomedical Research, Tohoku University, Japan as a frozen stock. Cells were adherently cultured in DMEM with 10% newborn calf serum (NCS), 1× GlutaMax, and 1× Antibiotic-Antimycotic (Invitrogen/Gibco) on normal tissue culture dishes (uncoated) at 37°C, 5% CO_2, which is referred to as normal conditions (NC).

Generation of neurosphere-like cells (Neurosphere assay)

Neurosphere assays were carried out according to previous studies (Das *et al.* 2006; Brewer & Torricelli 2007) with minimal modifications. Briefly, NIH/3T3 fibroblasts were cultured in suspension in NC or neural stem cell medium (NSCm) on 2.0% agarose-coated dishes at a density of 1×10^5 cells/mL for 5–7 days to detect the ability of these cells to form spheres. NSCm was serum-free and composed of DMEM/F-12, 1× GlutaMax, 1× Antibiotic-Antimycotic, 1× B27 supplement (without vitamin A: Cat. No. 12587), 1× N2 supplement, 20 ng/mL bFGF (basic fibroblast growth factor), and 20 ng/mL EGF (epidermal growth factor). All reagents were obtained from Invitrogen/Gibco. Adherent NIH/3T3 fibroblasts cultured in NC on normal tissue culture dishes were used as a control.

Passage of neurosphere-like cells

After 5–7 days of cultivation, spheres were trypsinized into single cells and resuspended in NSCm. The suspension was plated onto a new 2.0% agarose-coated dish and cultured for another 5–7 days to test the ability of these cells to form secondary spheres.

To examine the proliferative ability and expression of neural progenitor markers of NIH/3T3-derived spheres, after 7 days of floating cultivation for the second passage, the spheres were exposed to 10 μmol/L BrdU (Sigma) to tag the dividing cells and plated onto poly-D-lysine-coated 8-well culture slides (BD Biosciences) for the final 48 h (Das *et al.* 2006). Immunocytochemistry was carried out for double staining analysis of the neural progenitor markers Nestin, Sox2, Pax6, Musashi-1 (Msi1), and BrdU. RNA was isolated from NIH/3T3 cells cultured in different conditions, and real-time polymerase chain reaction (PCR) were performed to compare the expression of neural progenitor markers Nestin and Sox2.

Differentiation of neuron- and glia-like cells

For the differentiating culture, NSCm-cultured spheres were trypsinized into single cells and resuspended in differentiating medium (DM), then plated onto poly-D-lysine-coated 8-well culture slides and cultured for an additional 8 days. In DM, EGF and B-27 supplement (without RA Cat. No.12587) were replaced by 1% serum and standard B-27 supplement (including retinyl acetate: Cat. No. 17504). In addition, brain-derived neurotrophic factor (BDNF: 10 ng/mL) was added to promote the differentiation into neuronal cells, and ciliary neurotrophic factor (CNTF: 20 ng/mL) was added for glial cell differentiation (Yang *et al.* 2005; Das *et al.* 2006; Chen *et al.* 2007; Chojnacki & Weiss 2008; Matsuda *et al.* 2009). Immunocytochemistry was carried out to stain the markers of neurons (β-tubulin and neurofilament 200 [NF200]), astrocytes (glial fibrillary acidic protein [GFAP]), and oligodendrocytes (O4).

Induction of retinal photoreceptor-like cells

For the induction of retinal photoreceptor-like cells, NIH/3T3-derived neuron-like cells were trypsinized and